THE JOURNAL OF BIOLOGICAL CHEMISTRY VOL. 288, NO. 24, pp. 17313–17335, June 14, 2013

Tubulin Polymerization-promoting Protein (TPPP/p25α) Promotes Unconventional Secretion of α-Synuclein through Exophagy by Impairing Autophagosome-Lysosome Fusion*[S]

Received for publication, October 26, 2012, and in revised form, April 12, 2013 Published, JBC Papers in Press, April 29, 2013, DOI 10.1074/jbc.M112.401174

Patrick Ejlerskov[‡§], Izabela Rasmussen[‡], Troels Tolstrup Nielsen[‡¶], Ann-Louise Bergström[‖], Yumi Tohyama[**], Poul Henning Jensen[‡‡], and Frederik Vilhardt[‡1]

From the [‡]Department of Cellular and Molecular Medicine, The Panum Institute, University of Copenhagen, 2200 Copenhagen N, Denmark, the [§]Biotech Research and Innovation Centre, University of Copenhagen, 2200 Copenhagen N, Denmark, the [¶]Danish Dementia Research Centre, Department of Neurology, Rigshospitalet, Copenhagen University Hospital, 2100 Copenhagen, Denmark, [‖]Lundbeck A/S, 2500 Valby, Denmark, the [**]Division of Biochemistry, Faculty of Pharmaceutical Sciences, Himeji Dokkyo University 7-2-1 Kamiohno, Himeji, Hyogo 670-8524 Japan, and the [‡‡]Department of Biomedicine, Aarhus University, 8000 Aarhus, Denmark

Background: The mechanism of unconventional secretion of α-synuclein is unknown.
Results: Autophagy of α-synuclein followed by exocytosis of autophagy intermediates (exophagy) are increased by expression of TPPP/p25α.
Conclusion: Exophagy of α-synuclein is increased by lysosomal dysfunction and/or altered trafficking of autophagosomes.
Significance: Exophagy of α-synuclein might represent the first step in inter-neuronal spread of Lewy body disease.

Aggregation of α-synuclein can be promoted by the tubulin polymerization-promoting protein/p25α, which we have used here as a tool to study the role of autophagy in the clearance of α-synuclein. In NGF-differentiated PC12 catecholaminergic nerve cells, we show that *de novo* expressed p25α co-localizes with α-synuclein and causes its aggregation and distribution into autophagosomes. However, p25α also lowered the mobility of autophagosomes and hindered the final maturation of autophagosomes by preventing their fusion with lysosomes for the final degradation of α-synuclein. Instead, p25α caused a 4-fold increase in the basal level of α-synuclein secreted into the medium. Secretion was strictly dependent on autophagy and could be up-regulated (trehalose and Rab1A) or down-regulated (3-methyladenine and ATG5 shRNA) by enhancers or inhibitors of autophagy or by modulating minus-end-directed (HDAC6 shRNA) or plus-end-directed (Rab8) trafficking of autophagosomes along microtubules. Finally, we show in the absence of tubulin polymerization-promoting protein/p25α that α-synuclein release was modulated by dominant mutants of Rab27A, known to regulate exocytosis of late endosomal (and amphisomal) elements, and that both lysosomal fusion block and secretion of α-synuclein could be replicated by knockdown of the p25α target, HDAC6, the predominant cytosolic deacetylase in neurons. Our data indicate that unconventional secretion of α-synuclein can be mediated through exophagy and that factors, which increase the pool of autophagosomes/amphisomes (*e.g.* lysosomal disturbance) or alter the polarity of vesicular transport of autophagosomes on microtubules, can result in an increased release of α-synuclein monomer and aggregates to the surroundings.

Parkinson disease (PD)[2] is characterized by the progressive loss of dopaminergic neurons in the substantia nigra, although other neural populations of the central nervous system (CNS) are also affected. PD develops and progress over many years and affects an increasingly larger volume of the nervous system. Braak *et al.* (1) have hypothesized that progression of PD correlates with a topographical spreading pattern of α-synuclein inclusion body disease throughout the nervous system, which is also the case of spreading α-synucleinopathy induced by injection of preformed α-synuclein fibrils into the cortex or striatum of transgenic α-synuclein-expressing mice (2). However, despite demonstrations that neurons are capable of secreting and internalizing α-synuclein (3, 4), and that Lewy body pathology can be transferred from recipient to engrafted embryonic stem cells or fetal mesencephalic dopaminergic neurons in patients or experimental animals (5–7), little is known about the inter-neuronal transmission mechanisms of α-synuclein species.

Aggregated or modified forms of α-synuclein are degraded by proteasomal activity and different forms of autophagy (8, 9). During quality control (QC) macroautophagy a double-layered isolation membrane, also termed the phagophore, encloses a

* This work was supported by grants from the Danish Parkinson Foundation (to F. V. and P. E.), The JASCHA Foundation, The Warwara-Larsen Foundation, The Danish Research Council, Aase and Ejnar Danielsens Foundation, NOVO Nordisk Foundation (to F. V.), and the Lundbeck Foundation (to P. H. J.).
[S] This article contains supplemental Movie 1.
[1] To whom correspondence should be addressed: Dept. of Cellular and Molecular Medicine, Faculty of Health Sciences, Copenhagen University, The Panum Institute, 18.4, Blegdamsvej 3, 2200N Copenhagen, Denmark. Tel.: 45-35327120; E-mail: vilhardt@sund.ku.dk.

[2] The abbreviations used are: PD, Parkinson disease; TPPP, tubulin polymerization-promoting protein; QC, quality control; ATG, autophagy-related gene; eGFP, enhanced GFP; ROI, region of interest; pAb, polyclonal antibody; SNC, synuclein; PI, propidium iodide; mTOR, mammalian target of rapamycin; 3-MA, 3-methyladenine; IOD, integrated optical density.

volume of cytosol-containing damaged organelles or polyubiquitinated protein aggregates and thereby forms a vacuolar autophagosome (10). Generation of autophagosomes requires membrane lipids derived from endoplasmic reticulum, Golgi, or mitochondria (11) and is regulated by a set of conserved autophagy-related genes (ATG), including initiators (PI3K and Beclin-1) and elongators (conjugations systems ATG5–ATG12 and cytosolic light chain 3B (LC3B)) (12, 13). The autophagic vacuole then quickly matures by fusion with compartments of the endosomal pathway before final fusion with lysosomes to generate an autolysosome where the luminal content of the autophagosome is degraded (14). Specifically, the fusion organelle of an autophagosome and an endosome (often a multivesicular body) is called an amphisome. In contrast to starvation-induced autophagy, which indiscriminately encloses a volume of cytosol and organelles for degradation and recycling of protein-building blocks, QC autophagy typically accepts polyubiquitinated proteins, long lived proteins, aggregates, and organelles as cargo. Selectivity is provided by ubiquitin-binding adaptor proteins p62/SQSTM1, NBR1, and HDAC6 (15, 16), which link ubiquitinated cargo to LC3B, and in the case of HDAC6, additionally to dynein-dynactin motor proteins (16–20). Neurons depend on autophagy for differentiation and survival (21), and p62/SQSTM1 and HDAC6 are required for development of inclusion bodies and aggresomes by directing minus-end transport of ubiquitinated cargo on microtubuli (15, 16).

Lewy bodies invariably contain modified and aggregated α-synuclein as the main component along with a number of other nerve cell proteins typically highly ubiquitinated. The tendency of α-synuclein to form cytosolic aggregates is influenced by a number of other proteins, including synphilin-1 (22), protein interacting with NIMA 1 (PIN-1) (23), and TPPP/p25α (hereafter referred to as p25α) (24). The p25α protein binds to microtubules and by doing so lowers their plus-end growth rate and protects them from depolymerization (25–27). In addition, p25α potently stimulates aggregation of α-synuclein *in vitro* and localizes to Lewy bodies *in vivo* (24, 28). In the CNS, p25α is mainly expressed in oligodendrocytes and is required for their differentiation (29), but during PD progression p25α becomes ectopically expressed in dopaminergic neurons. Conversely, α-synuclein is up-regulated in p25α-expressing oligodendrocytes of patients with multiple system atrophy (24), and both proteins co-localize in characteristic inclusion bodies of these diseases.

In this study, we have asked the question whether α-synuclein species can be secreted by dopaminergic neurons following autophagy and exophagy. For this purpose, we have used the well known PC12 pheochromocytoma cell line as a model system of dopaminergic neuron-like cells to conditionally express the aggregation-prone α-synuclein$_{A30P}$ protein with or without p25α as a tool to increase α-synuclein aggregation and autophagic uptake. We show here that α-synuclein monomer and high molecular weight species can be secreted by exophagy and that p25α further augments this process by inhibiting autophagosomal fusion with lysosomes.

MATERIALS AND METHODS

Cell Culture and Neuronal Differentiation—The rat pheochromocytoma cell line PC12 (ATCC) was seeded on collagen-coated culture dishes and cultured in DMEM containing 10% horse serum, 5% fetal calf serum, and 1% penicillin and streptomycin at 37 °C in 5% CO_2. For experiments, PC12 cells were seeded at a density of 45,000 cells/cm^2 and differentiated in DMEM containing 2% horse serum, 1% penicillin and streptomycin, and 100 ng/ml nerve growth factor (NGF) (2.5S subunit, Serotec) for 2 days before transgene expression was induced for an additional 2 days with doxycycline (200 ng/ml). SH-SY5Y cells were cultured in DMEM containing 10% fetal calf serum and 1% penicillin and streptomycin at 37 °C in 5% CO_2. For experiments, SH-SY5Y cells were differentiated with 10 μM all-*trans*-retinoic acid for 6–8 days to obtain a neuron-like phenotype before transgene expression was induced by treatment with doxycycline (200 ng/ml) for an additional 24 h.

Antibodies and Chemical Reagents—Antibodies used include mouse anti-α-synuclein mAb from BD Transduction Laboratories, mouse anti-α-synuclein mAb (LB509) from Abcam, rabbit anti-α-synuclein mAb (EP1646Y) from Abcam, and rabbit anti-α-synuclein polyclonal antibody from Sigma. Rabbit anti-LC3B and anti-p62/SQSTM1 pAbs, mouse anti-acetylated tubulin mAb, and mouse anti-β-actin mAb were from Sigma; rabbit anti-p25α pAb was from Novus; rat anti-TPPP/p25α mAb was from Enzo Life Sciences; rabbit anti-cleaved caspase-3 pAb (D175) and mouse anti-ubiquitin mAb were from Cell Signaling; rabbit anti-LAMP1 pAb was from Novus; mouse anti-HA mAb was from Santa Cruz Biotechnology; rabbit anti-GFP pAb was from Molecular Probes); and mouse anti-ubiquitin mAb was from Novus Biologicals. Alexa 488- or 568-conjugated annexin-V, Alexa-conjugated phalloidin, and Alexa 488-, 568-, or 633-conjugated goat anti-mouse or -rabbit antibodies were from Molecular Probes; horseradish peroxidase (HRP)-conjugated swine or goat anti-mouse or rabbit secondary antibodies was from DAKO; ToPro-3 iodide was from Molecular Probes for nucleus staining. The following chemicals were used: bafilomycin A1; leupeptin; pepstatin A; trichostatin A; trehalose; HEPES; trichloroacetic acid (TCA); Triton X-100, Tween 20; phosphatase and protease inhibitor mixture; (all from Sigma); and 3-MA (from Calbiochem).

Lentivector Construction and Transduction—For conditional expression of transgenes, cDNAs were PCR-cloned into BamHI/SalI-restricted lentiviral vector pLOX-cPPT.TW.W expressing cDNA under the control of a tetracycline-responsive promoter (Tet-On). Already established and tested PC12-rtTA or SH-SY5Y-rtTA cell lines expressing the reverse tetracycline-controlled transactivator (rtTA) were superinfected with pLOX-cPPT.TW.W lentivectors expressing the cDNAs of β-synuclein, α-synuclein$_{wt}$, α-synuclein$_{A30P}$, or p25α or with the pHR-cPPT.CMV.W lentivector for constitutive expression of mCherry-eGFP-LC3B (kindly provided by Professor Terje Johansen, Institute of Medical Biology, University of Tromsø, Norway (20)); 3×HA-tagged Rab1A, Rab3A, or Rab8 (all human cDNAs from Missouri S&T cDNA Resource Center); or Rab7-GFP fusion constructs alone or in combination as specified. Dominant negative and positive Rab27A mutants Rab27A-

T23N and Rab27A-Q78L, respectively, were expressed under the control of a CMV promoter in the pLenti6-V5-TOPO vector (30). For expression of polyglutamine tracts from exon 1 of human huntingtin, templates contained in plasmids pEGFP/HD-120Q and pEGFP/HD-18Q (31) were subcloned into the plasmid PCR2.1 (Invitrogen) by PCR using primers 5′-GGA TCC ATT CAT TGC CCC GGT GCT G-3′ and 5′-GGA TCC CCG GCT GAG GAA GCT GAG GAG-3′ and then BamHI cloned into the pHR-cPPT.CMV.GFP.W vector to express huntingtin-115Q-GFP or -18Q-GFP. All constructs were verified by sequencing. Knockdown of HDAC6 expression was carried out by transducing PC12 cells 72 h prior to analysis with Sigma MISSION™ HDAC6 shRNA in a pLKO.1 lentivector backbone (sense sequence AGGAAAGGTTCTCGAAGCA). PC12 cell populations knocked down for ATG5 were generated by the combined constitutive expression of two ATG5 shRNAs (sense sequence, CTTGGAACATCACAGTACA and CTGTTTACAGTCAGTCTAT) contained in the pGIPZ lentivector (Open Biosystems). At least 85% of cells carried transgenes (conditionally or constitutively) following creation of stable PC12 populations by lentiviral transduction, whereas transduction of differentiating PC12 cells yielded transduction efficiencies ranging from 40 to 60%. Vector production was carried out as described previously (32).

Western Blotting—Cells were lysed in lysis buffer (100 mM NaCl, 50 mM Tris-HCl, 1 mM EGTA, 10 mM $MgCl_2$, pH 7.2) containing 1% Triton X-100, phosphatase, and protease inhibitor mixture for 5 min at room temperature and thereafter kept on ice. Cell lysates were centrifuged at 16,100 × *g* for 5 min at 4 °C, and protein concentrations of the supernatant were determined with D_c protein assay (Bio-Rad), before addition of Laemmli buffer and loading of equivalent protein quantities on SDS-polyacrylamide gels for Western blotting using chemiluminescent HRP detection substrate (Millipore).

TCA Protein Precipitation—Conditioned medium was harvested and centrifuged at 800 × *g* for 5 min, 4 °C, before ice-cold TCA was added to the supernatant and incubated on ice for 10 min. The protein precipitates were pelleted by centrifugation (16,100 × *g*, 5 min, 4 °C) and washed 4–5 times in ice-cold acetone until the pellet appeared clear white. The pellets were dried at 95 °C for 10 min, dissolved in 2.5× Laemmli buffer, boiled for 20 min at 95 °C, and subsequently processed for Western blotting.

Exosome Preparation—Conditioned medium from 10-cm Petri dishes with either PC12-α-synuclein$_{A30P}$ or α-synuclein$_{A30P}$/p25α cells was pre-centrifuged at 1,200 × *g* for 10 min followed by another round of centrifugation at 10,000 × *g* for 30 min. The supernatants were then passed through 0.22-μm filters before centrifugation at 100,000 × *g* for 1 h in a Beckman centrifuge with SW40Ti rotor. The pellet containing exosomes was washed once in PBS, and then aliquots of pellet and supernatant were separated by gel electrophoresis and processed for Western blotting.

Homogenization and Sucrose Gradient Fractionation—PC12 cells were suspended in PBS^- and pelleted by centrifugation at 800 × *g* for 8 min, 4 °C. Cells were washed once in hypotonic buffer (170 mM sucrose, 75 mM NaCl, and 10 mM HEPES, pH 7.0) containing protease and phosphatase inhibitor mixture, snap-frozen in liquid nitrogen, re-thawed in 200 μl of hypotonic buffer, and then repeatedly aspirated with a 27-gauge needle. The volume was diluted to 500 μl with hypotonic buffer before centrifugation at 800 × *g* for 8 min, 4 °C. Subsequently, the supernatant was centrifuged at 10,000 × *g* for 10 min, 4 °C. The post-nuclear/mitochondrial supernatant was then applied to the top of a 15–45% sucrose gradient in gradient buffer (140 mM NaCl, 25 mM HEPES, pH 7.2) and ultracentrifuged in a Beckman centrifuge with an SW40Ti rotor head at 30,000 rpm for 18 h, 4 °C. Twelve 1-ml fractions were collected from the bottom with a peristaltic pump, and aliquots thereof were processed for Western blotting.

Immunofluorescence and Electron Microscopy—PC12 cells were washed once in Hanks' balanced saline solution and fixed in a phosphate buffer containing 2% paraformaldehyde, pH 7.4, for 30 min. Immunofluorescence was essentially performed as described previously (33), and images were acquired with a Zeiss LSM510 confocal laser scanning microscope with a C-Apochromat ×63, 1.4 NA oil immersion objective, using the argon 488-nm and the helium/neon 543- and 633-nm laser lines for excitation of Alexa 488, 568, and 633, respectively. Confocal sections of 0.8–1.0 μm were collected and saved as 512 × 512-pixel or 1024 × 1024-pixel images at 12-bit resolution before import to Adobe Photoshop CS2 version 9.0.2, Zeiss LSM image browser, or ImageJ for compilation and quantification. When quantifying apoptotic cells, 8–12 images (each containing around 200 cells) were acquired for each condition with a Fluar ×20, 0.75 NA water immersion objective. Cells positive for cleaved caspase-3 and the total number of cells (identified by ToPro-3 iodide) were quantified by a custom-made macro in ImageJ. For ultrastructural analysis, PC12 cells were fixed in a phosphate buffer containing 2% paraformaldehyde and 0.2% glutaraldehyde, pH 7.4, and processed for either Epon embedding or cryopreservation and sectioning as described previously (33). Cryo-EM sections were incubated with monoclonal mouse anti-α-synuclein mAb LB509 and polyclonal rabbit anti-GFP (A64655, Molecular Probes) followed by 7- and then 14-nm gold-conjugated goat anti-mouse or -rabbit antibodies, respectively. Sections were examined in a Phillips CM 100 electron microscope equipped with a digital camera.

Fluorescence Recovery after Photobleaching (FRAP)—PC12 cells expressing mCherry-eGFP-LC3B were imaged in HEPES buffer, pH 7.4, 37 °C. A circular region of interest (ROI) measuring 35 pixels in diameter was defined, and after three initial images mCherry fluorescence in the ROI was bleached with the 543-nm laser (30 iterations, at 100% laser strength). Subsequently, fluorescence recovery in the ROI was measured over a period of 3.5 min every 10th second. The fluorescence recovery was adjusted for general photobleaching. Eight to ten cells were measured for each experiment, and mean values were acquired from a minimum of three independent experiments.

FACS Analysis—For cell death analysis, PC12 cells were differentiated in 12-well culture plates and then were incubated with 2 μg/ml propidium iodide (PI) for 15 min at RT and subsequently placed on ice. The cells were immediately analyzed in an Accuri C6 flow cytometer using the 488-nm laser for excitation and the FL3 optical filter (>670 nm) for emission detection. The fluorescence limit defining PI-positive cells was set

based on control PC12 cells that did not receive PI. When analyzing the endosomal degradation pathway, PC12 cells were incubated with 40 μg/ml bovine serum albumin (BSA) conjugated to the green fluorescent BODIPY FL dye (DQ-BSA) (Molecular Probes) for 6.5 h prior to flow cytometric analysis using the FITC filter. Mean fluorescence intensity of cells that did not receive DQ-BSA was subtracted from all sample values.

Statistical Analysis—Data were analyzed with one-way analysis of variance or Student's *t* test, and significance levels were defined as *p* values less than 0.05 (* or #), 0.01 (** or ##), or 0.001 (*** or ###). The largest and the smallest variances were tested for homogeneity with *F*-test before testing. Bar graph values are expressed as means and error bars as means ± S.E.

RESULTS

Expression of p25α Inhibits Neurite Extension and Degradative Capacity of PC12 Cells—We used lentiviral transduction to obtain conditional (Tet-On) expression of α-synuclein$_{wt}$ or mutant α-synuclein$_{A30P}$ with or without co-expression of p25α in PC12 pheochromocytoma cells differentiated to catecholaminergic nerve cells with NGF. Unless otherwise specified, we adopted a differentiation protocol consisting of 2 days of pretreatment with NGF followed by 2 days of NGF and doxycycline treatment for transgene expression. At this time cells expressing α-synuclein, or control cells expressing the nonpathogenic but closely related β-synuclein, formed a fully extended neurite network (Fig. 1*A*), although α-synuclein expression, in particular α-synuclein$_{A30P}$, caused α-synuclein-positive neurite blebs (Fig. 1*B, arrowheads*). In contrast, p25α expression alone or in combination with α-synuclein caused cell flattening and impaired neurite growth (Fig. 1, *A* and *B*). The Tet-On system provided an equal expression level of transgenes in PC12 cells with only minor leakage from the promoter (Fig. 1*C*). The anti-α-synuclein antibodies used throughout this study, unless otherwise stated, react only weakly with endogenous rat α-synuclein in Western blotting applications. However, an alternative α-synuclein mAb (Abcam EP1646Y) with higher affinity to rat α-synuclein detects endogenous rat α-synuclein, and (with the limitations of cross-species antibody detection) we estimate that PC12 cells differentiated with NGF for 4 days express transgene α-synuclein$_{A30P}$ ~50-fold higher than the endogenous level of α-synuclein after 48 h of doxycycline induction. Of note, differentiated PC12 cells express considerably lower levels of α-synuclein than primary nerve cells from mouse (data not shown). TPPP/p25α expression is usually absent in cell lines, and we could not detect it in PC12 cells. All Western blot data in the following pertain to transgene α-synuclein, although endogenous α-synuclein is also recruited (see Fig. 4, *C–E*). Lowering the serum concentration to initiate NGF-induced differentiation causes roughly 15% of β-synuclein-expressing control cells to die, but within the time frame, α-synuclein and p25α co-expression only further augmented cell death through apoptosis by roughly 3% (Fig. 1, *D* and *E*). Huntingtin containing pathological polyglutamine stretches is a substrate of both the proteasomal and autophagosomal degradation pathways, which both are known to be inhibited by modified forms of α-synuclein (34–36). Failure to degrade huntingtin results in the formation of large inclusion bodies called aggresomes. We therefore tested the effect of α-synuclein and/or p25α expression on the ability of PC12 cells to deal with co-expression of a polyglutamine tract (Gln-115) from huntingtin fused to GFP, or as control the nonpathogenic Gln-18-GFP. As illustrated in Fig. 1, *F* and *G*, expression of either α-synuclein$_{A30P}$ or p25α alone or in combination increased huntingtin inclusion body formation up to 2-fold, indicating that p25α and α-synuclein$_{A30P}$ expression interferes with the degradative machinery of the cells.

Expression of p25α Redistributes α-Synuclein to Cytosolic Vesicles and Causes Increased Autophagy—The majority of PC12 cells expressing α-synuclein$_{wt}$ or α-synuclein$_{A30P}$ had a compact cell body, and α-synuclein was distributed mainly in the cell periphery and in neurites, whereas p25α had a more diffuse somatic distribution (Figs. 1*B* and 2, *A* and *B*). In contrast, when co-expressed, p25α co-localized closely with α-synuclein$_{A30P}$ and induced its redistribution into cytosolic aggregates, inclusions, and/or vesicles (Fig. 2*C*). In a subset of PC12-α-synuclein$_{A30P}$/p25α cells (around 5%), large inclusion bodies with diameters up to 5 μm could be observed (Fig. 2*D*). PC12 cells expressing α-synuclein alone did not contain any distinguishable inclusion bodies (Fig. 2*A*). α-Synuclein and its mutant forms are known to be degraded by macroautophagy (henceforth "autophagy") and chaperone-mediated autophagy (8, 9), and neurons are dependent on basal autophagy (21, 36). We therefore analyzed conversion of the autophagosomal adaptor protein LC3B in differentiated PC12 cells. A minor significant increase was observed in α-synuclein-expressing PC12 cells, but p25α expression markedly increased conversion of LC3B-I (cytosolic; upper band in Western blots) to LC3B-II (autophagosome membrane-conjugated; lower band) (Fig. 2, *E* and *F*). Also, an ~3-fold increase in the LC3B-II/LC3B-I ratio was observed in differentiated SH-SY5Y cells expressing α-synuclein$_{A30P}$ with p25α (Fig. 2, *G* and *H*). We next subjected the cells to ultrastructural analysis to confirm an increased autophagic flux (Fig. 2, *I–N*). Co-expression of p25α increased the number of nascent autophagosomes in α-synuclein-expressing PC12 cells (Fig. 2, *I, M, J–L,* and *O, black, open arrows*), which correlated with an increased number of amphisomes, clearly containing luminal vesicles derived from fusion with late endosomes (Fig. 2, *M* and *N, white filled arrows,* shows the fusion of a late endosome and an autophagosome to form an amphisome), and multilamellar bodies containing whorls of partially degraded lipids (Fig. 2*M, white open arrows*). Autophagosomes were evident in all parts of soma as well as neurites, and autophagosomes were observed to sequester various organelles, including endosomes, dense core vesicles, and mitochondria (Fig. 2, *J–L*).

α-Synuclein$_{A30P}$ Co-localizes with Markers of Autophagosomes—To further pursue the involvement of autophagosomal protein clearance, we chose to focus on the aggregation prone mutant α-synuclein$_{A30P}$, which is a more likely substrate for QC autophagy than α-synuclein$_{wt}$. By indirect immunofluorescence of PC12 cells expressing α-synuclein$_{A30P}$, we only observed few vesicular structures with overlapping fluorescence between α-synuclein$_{A30P}$ and the autophagosomal markers LC3B (Fig. 3*A, arrow*). This co-localization was increased considerably by co-expression of p25α, which also to a lesser

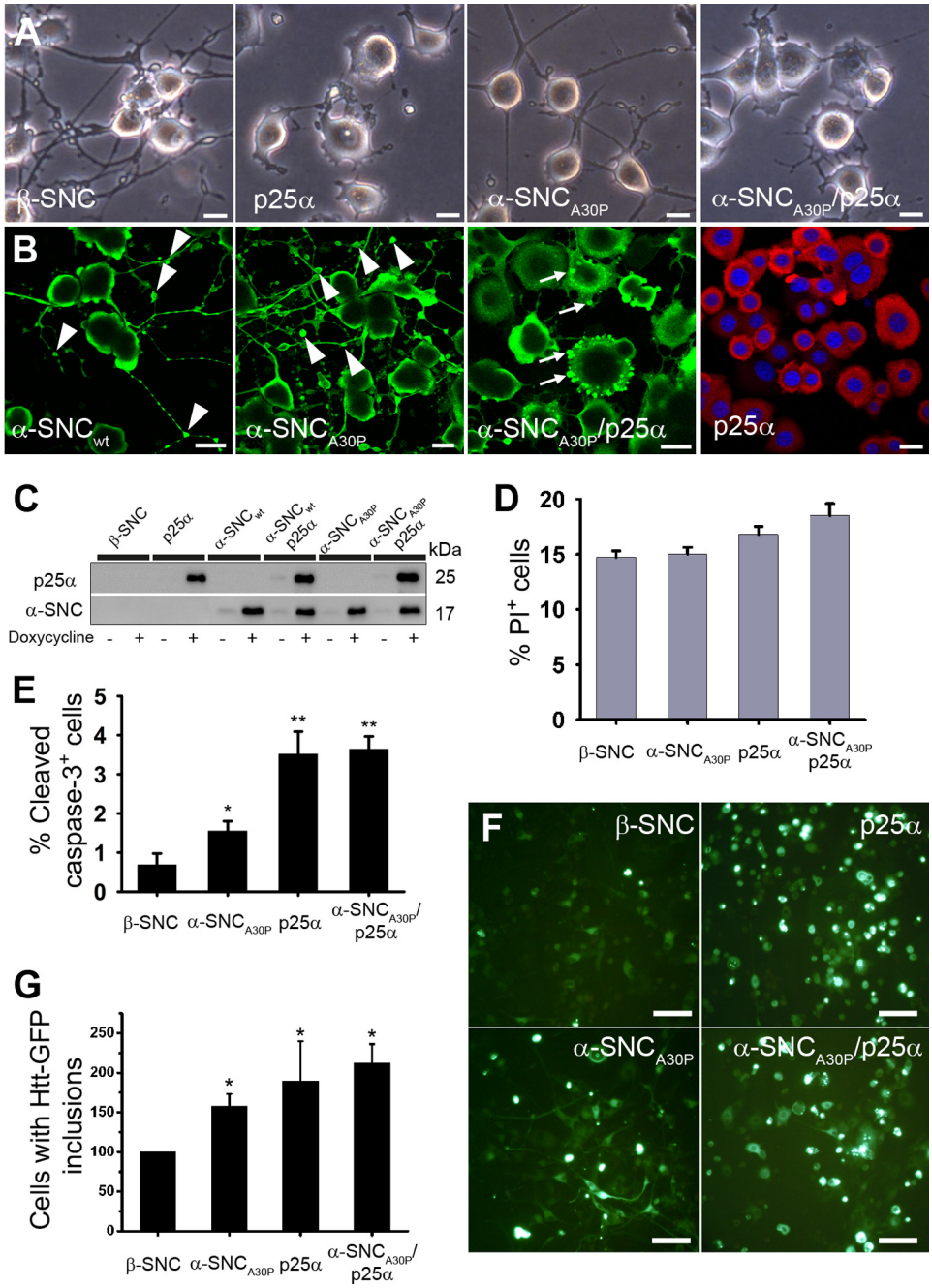

FIGURE 1. **Conditional expression of p25α and α-synuclein in NGF-differentiated PC12 nerve cells.** PC12 cells were predifferentiated with 100 ng/ml NGF for 2 days, and then transgene expression of β-synuclein (*β-SNC*), p25α, α-synuclein$_{wt}$ (*α-SNC$_{wt}$*), α-synuclein$_{A30P}$ (*α-SNC$_{A30P}$*), or α-SNC$_{A30P}$ and p25α was induced by doxycycline treatment for additionally 2 days. *A,* bright field images showing p25α-mediated impairment of neurite outgrowth. *Bars,* 20 μm. *B,* indirect immunofluorescence of PC12 cells expressing α-SNC$_{wt}$, α-SNC$_{A30P}$, α-SNC$_{A30P}$/p25α, or p25α alone with antibodies against α-SNC (BD Transduction Laboratories) (*green*) or p25α (*red*). *Arrowheads* indicate neurite blebbing, and *arrows* indicate α-SNC-positive inclusions. *Bars,* 20 μm. *C,* representative Western blots of transgene expression in doxycycline-treated or -nontreated PC12 cell lines analyzed with antibodies against p25α and α-SNC (BD Transduction Laboratories) as indicated. *D,* flow cytometry analysis of PI uptake as a measurement of cell death. The *graph* shows mean ± S.E. of PI-positive cells as a percentage of the whole population ($n = 3$). *E,* quantitation of caspase-3-positive cells detected by indirect immunofluorescence and counting. The *bar graph* shows mean ± S.E. values as percentage caspase-3-positive cells of the whole population ($n = 3$). *F,* differentiated PC12 cells lines were transduced with a lentivector expressing a pathogenic polyglutamine tract from exon 1 of huntingtin fused to GFP (Htt-115Q-GFP) and then induced with doxycycline. The images show microscopic fields containing ~50 cells, whereof a proportion is highly fluorescent due to inclusion body formation. *Bar,* 100 μm. *G, bar graph* shows the number of PC12 cells per microscopic field containing Htt-115Q-GFP inclusion bodies after 4 days, normalized to PC12 cells co-expressing β-synuclein (*β-SNC*). The data represent mean ± S.E. from three independent experiments.

degree caused co-localization of α-synuclein$_{A30P}$ and the autophagosomal adaptor protein p62/SQSTM1 (Fig. 3, *B* and *C, arrows*), indicating that p25α substantially increases the suitability of α-synuclein as an autophagosomal substrate. We verified these light microscopic observations by cryo-immunogold labeling for EM, and for this purpose we made use of PC12 cells constitutively expressing an mCherry-eGFP-LC3B fusion construct (20). α-Synuclein detected by the monoclonal antibody LB509 could be co-localized with LC3B (detected with anti-GFP antibody) in autophagosomes in both PC12-α-

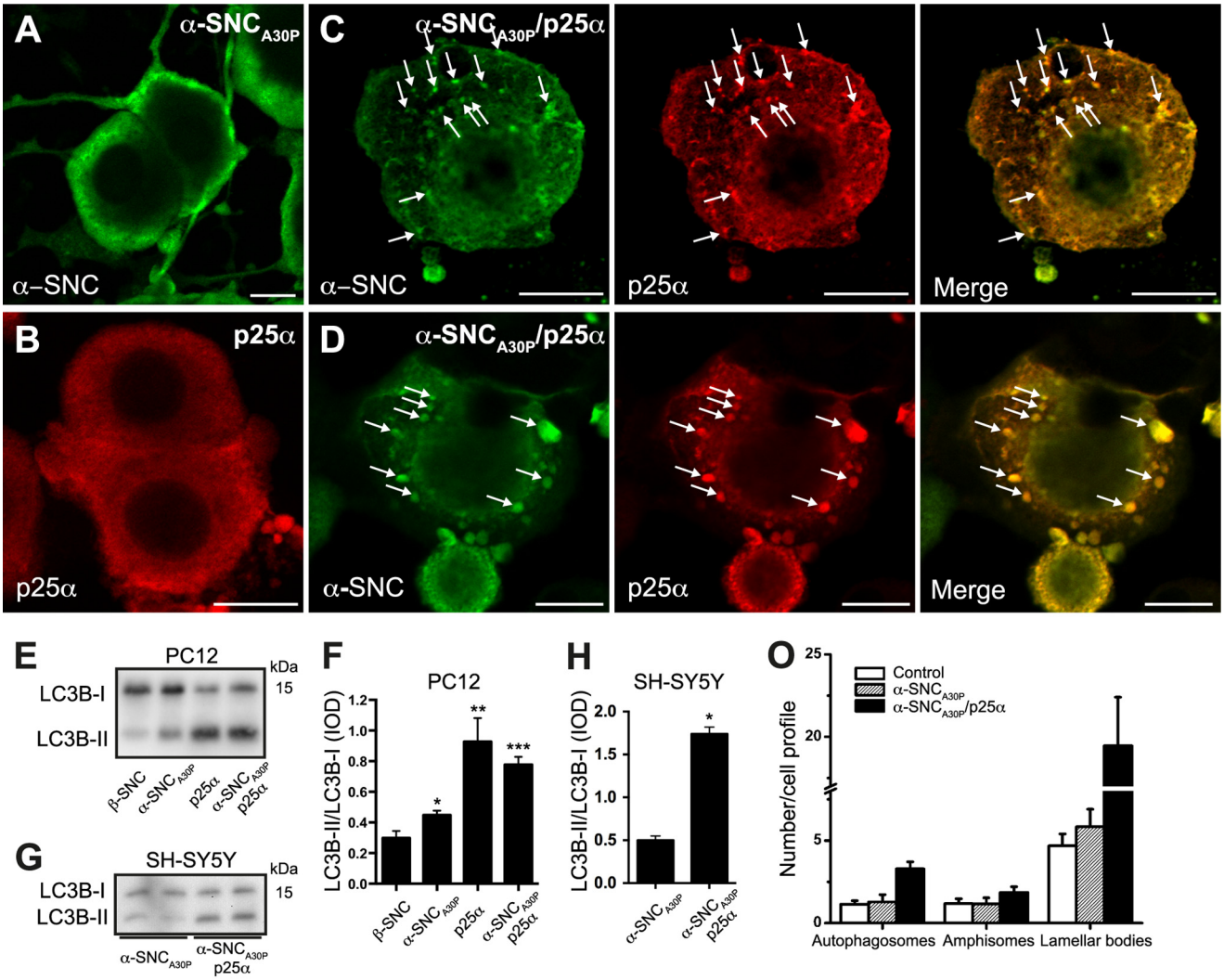
A
α-SNC$_{A30P}$
α–SNC
C
α-SNC$_{A30P}$/p25α
α–SNC
p25α
Merge
B
p25α
p25α
D
α-SNC$_{A30P}$/p25α
α-SNC
p25α
Merge
E
PC12
kDa
15
LC3B-I
LC3B-II
β-SNC
α-SNC$_{A30P}$
p25α
α-SNC$_{A30P}$ p25α
F
PC12
LC3B-II/LC3B-I (IOD)
1.2
1.0
0.8
0.6
0.4
0.2
0.0
**
*
***
β-SNC
α-SNC$_{A30P}$
p25α
α-SNC$_{A30P}$ p25α
G
SH-SY5Y
kDa
15
LC3B-I
LC3B-II
α-SNC$_{A30P}$
α-SNC$_{A30P}$ p25α
H
SH-SY5Y
LC3B-II/LC3B-I (IOD)
2.0
1.5
1.0
0.5
0.0
*
α-SNC$_{A30P}$
α-SNC$_{A30P}$ p25α
O
Control
α-SNC$_{A30P}$
α-SNC$_{A30P}$/p25α
Number/cell profile
25
20
5
0
Autophagosomes
Amphisomes
Lamellar bodies

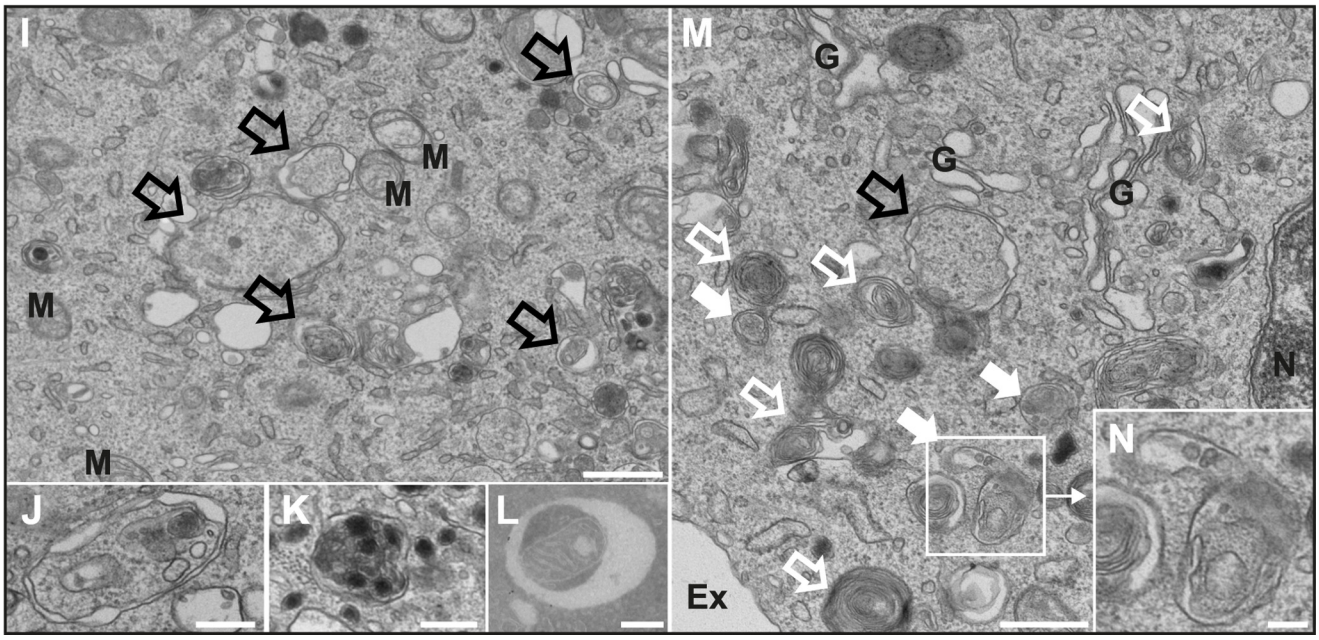
I
M
M
M
M
J
K
L
M
G
G
G
N
N
Ex

synuclein$_{A30P}$ (Fig. 3, *D–F*) and to a higher extent in α-synuclein$_{A30P}$/p25α-expressing cells (Fig. 3, *G–I*). In PC12-α-synuclein$_{A30P}$ cells, α-synuclein reactivity could also be detected in unidentified compartments without LC3B labeling (Fig. 3*F, black filled arrow*). In addition, α-synuclein and LC3B co-localized, in particular in PC12-α-synuclein$_{A30P}$/p25α cells, in matured autophagosomal elements, likely representing amphisomes (Fig. 3, *E*, *G,* and *H*; *white open arrows*). For reasons discussed below, we also consider (LC3B-positive) multilamellar bodies (Fig. 3*G, white open arrow*) as amphisomes, although in the absence of functional antibodies for cryo-EM labeling of rat late endosomal markers we cannot conclusively say so. Cells expressing β-synuclein yielded only very sparse nonspecific labeling (data not shown). Collectively, the data demonstrate that in the presence of p25α expression, overexpressed α-synuclein$_{A30P}$ becomes a suitable substrate for autophagy.

Expression of p25α Induces Selective Autophagy of α-Synuclein$_{A30P}$ and Also Affects Endogenously Expressed α-Synuclein—The p25α-mediated inclusion of α-synuclein into autophagosomes was selective, inasmuch as pathogenic Htt-115Q co-expressed in the same cells segregated entirely to p62/SQSTM1-positive aggresomes (Fig. 4, *A* and *B*). To rule out that the observed aggregation and autophagy of α-synuclein in the presence of p25α was due to overexpression of α-synuclein$_{A30P}$, we also studied the effects on endogenous rat α-synuclein in PC12 cells expressing only p25α by immunofluorescence. As shown in Fig. 4, *C* and *D*, p25α caused a marked redistribution of endogenous α-synuclein from the cell periphery into ubiquitin-positive structures, which in themselves increased in numbers compared with control cells expressing β-synuclein. These structures were also immunoreactive for p25α, as well as late endosome/amphisome markers KAI1 and mannose phosphate receptor (Fig. 4*E*).

α-Synuclein$_{A30P}$ Is Excluded from Lysosomes in p25α-expressing Cells—By immunofluorescence we observed considerable co-localization between α-synuclein and lysosome-associated membrane protein 1 (LAMP1) in α-synuclein$_{A30P}$-expressing PC12 cells after treatment with protease inhibitors leupeptin and pepstatin A (Fig. 5, *arrows*), indicating that vesicular α-synuclein observed by immunofluorescence and cryo-immunogold labeling eventually is degraded in lysosomes. However, in PC12 cells co-expressing p25α, α-synuclein$_{A30P}$-positive vesicles and inclusions were conspicuously devoid of LAMP1 immunoreactivity suggesting impaired fusion of amphisomes with lysosomes (Fig. 5, *B* and *C*). Although some LAMP1-positive lysosomes (Fig. 5*B, red arrows*) were distributed in close proximity to α-synuclein-positive vesicles (Fig. 5*B, green arrows*), there was no evident overlap, and this was also the case for larger inclusion bodies (Fig. 5*C, white arrows*). To substantiate this further, we first fractionated homogenates from α-synuclein$_{A30P}$- and α-synuclein$_{A30P}$/p25α-expressing PC12 cells on sucrose gradients by velocity centrifugation. Most α-synuclein$_{A30P}$ was contained within low density fractions (10–12) of the gradient corresponding to cytosolic proteins, including LC3B-I, and low density membrane (Fig. 5*D*). In PC12 cells expressing α-synuclein$_{A30P}$, a small accumulation of α-synuclein could be detected in the high density fractions (1–4) of the gradient corresponding to where lysosomes sediment (we were not able to identify a functional anti-rat LAMP antibody for Western blotting). These fractions contained only the LC3B-II form, which is incorporated into the membrane of autophagosomes. However, the high density fraction content of α-synuclein was diminished in PC12 cells co-expressing p25α (Fig. 5*D*). In addition, we performed a functional assay to investigate endosomal trafficking to lysosomes by incubating PC12 cells with fluorophore-conjugated BSA (DQ-BSA), which is internalized by endocytosis and becomes fluorescent only upon lysosomal proteolysis. Although PC12 cells expressing β-synuclein or α-synuclein$_{A30P}$ showed a similar proficiency in DQ-BSA degradation, expression of p25α alone or in combination with α-synuclein$_{A30P}$ decreased the level of DQ-BSA fluorescence (Fig. 5*E*). More dramatic decreases, which were largely cell line-independent, were obtained by either blocking lysosomal proteolysis with leupeptin/pepstatin A or by blocking fusion of late endosomes/amphisomes with lysosomes using the V-ATPase inhibitor bafilomycin A1, which inhibits endosomal and lysosomal acidification. Collectively, the results indicate that p25α impairs the delivery of α-synuclein to lysosomes by interfering with the fusion of autophagosome maturation intermediates including amphisomes with lysosomes.

Co-expression of p25α Impairs Autophagosome Maturation—We next analyzed the autophagosomal flux in greater detail by

FIGURE 2. **Expression of p25α promotes formation of α-synuclein-positive inclusions and alters the levels of proteins involved in autophagy.** *A–D,* indirect immunofluorescence of α-synuclein (*α-SNC*) (BD Transduction Laboratories) and p25α in NGF-differentiated PC12 cells expressing the following: *A*, α-SNC$_{A30P}$; *B,* p25α; or *C* and *D,* co-expressing α-SNC$_{A30P}$ and p25α. Note the pronounced co-localization between α-SNC and p25α (*arrows*) in both small vesicular profiles (*C*) and large inclusions (*D*). *Bars*, 10 μm. *E,* PC12 cell populations, as indicated, were differentiated as above, and cell lysates were processed for Western blotting with anti-LC3B antibodies. *F, bar graph* shows integrated optical density (*IOD*) ratio between Western blot bands of LC3B-II and LC3B-I obtained from seven independent experiments. *Error bars,* S.E. *G,* representative Western blot of all-*trans*-retinoic acid-differentiated SH-SY5Y cells expressing α-SNC$_{A30P}$ or α-SNC$_{A30P}$/p25α using anti-LC3B antibodies. *H, bar graph* shows integrated optical density ratio between Western blot bands of LC3B-II and LC3B-I obtained from three independent experiments. *Error bars*, S.E. *I–N,* PC12 cells expressing α-SNC$_{A30P}$/p25α were fixed and processed for EM. Shown are micrographs of Epon-embedded sections. *I,* area of the cell with many nascent autophagosomes (*black open arrows*) characterized by two outer membranes and a luminal content with an appearance very similar to cytosol. *M,* mitochondria. *Bar,* 500 nm. *J–L,* examples of autophagosomes containing different kinds of cargo, including cytosol with endosomes (*J*), several dense-core vesicles contained in an amphisome located in a dendrite (*K*), and mitochondria (*L*) as revealed by this cryo-EM section. *Bars, J–L*, 250 nm. *M,* area with many autophagosome intermediates. Amphisomes, which have recently fused with late endosomes (*white filled arrows*), are characterized by an outer membrane enclosing an autophagosomal body with limiting membrane in addition to material derived from fusion with endosomes (typically exosomes). In addition, many electron dense, multilamellar bodies containing whorls of lipid were observed, often in addition to identifiable autophagosomal material (*white open arrows*). A single nascent autophagosome is present (*black open arrow*) close to the Golgi apparatus (*G*), nucleus (*N*), and the extracellular space (*Ex*). *Bar,* 500 nm. *Inset, N* shows a fusion event between a late endosome and an autophagosome. *Bar,* 100 nm. *O, bar graph* shows mean ± S.E. of the number of autophagosomes, amphisomes, and lamellar bodies in PC12 cells expressing either the doxycycline-binding reverse tetracycline-inducible transactivator (*rtTA*) protein alone (*control*) or together with α-SNC$_{A30P}$ or α-SNC$_{A30P}$/p25α. From three independent EM experiments at least 10 cell profiles of each cell population were counted.

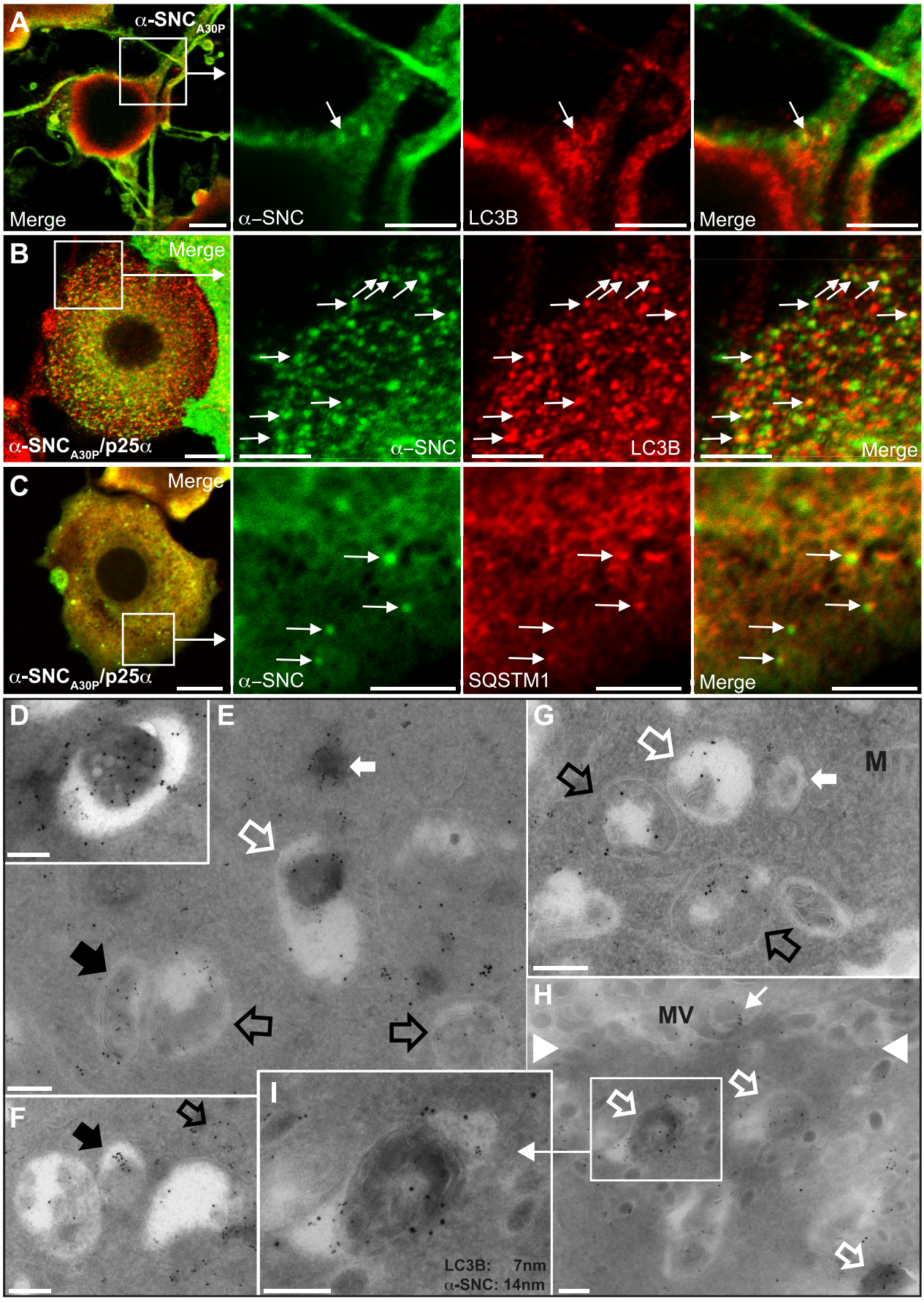
A
α-SNC A30P
Merge
α–SNC
LC3B
Merge
B
Merge
α-SNC A30P/p25α
α–SNC
LC3B
Merge
C
Merge
α-SNC A30P/p25α
α–SNC
SQSTM1
Merge
D
E
G
M
H
MV
F
I
LC3B: 7nm
α-SNC: 14nm

superinfecting PC12 cell lines with lentivector expressing the mCherry-eGFP-LC3B tandem construct (20). The construct is incorporated into the outer and inner leaflet of the isolation membrane of forming autophagosomes via LC3B. Although eGFP fluorescence is pH-sensitive and decreases upon fusion with low pH lysosomes, the mCherry fluorophore is pH-insensitive, which enables distinction of recently formed autophagosomes (co-localizing *green* and *red dots*) and autophagosomes, which have matured by fusion with lysosomes to form autolysosomes (only red dots). In PC12 cells expressing β-synuclein, ~80% of vesicular LC3B was associated with exclusively red dots indicating a continuous flux of autophagosomes that fuse with lysosomes (Fig. 6, *A*, *F,* and *G*). However, the ratio between mCherry- and mCherry/eGFP-positive vesicular compartments was decreased by both α-synuclein$_{A30P}$ and in particular p25α, indicating an impairment of the autophagosomal flux, which could be mimicked in PC12 β-synuclein cells by treatment with bafilomycin A1 (Fig. 6, *B*, *C,* and *E–G*). PC12 cells expressing p25α alone or together with α-synuclein$_{A30P}$ furthermore displayed large autophagosomes/amphisomes (>1 μm), and a subset of cells (2%) displayed structures with diameters ranging up to 5 μm (Fig. 6, *D* and *H*). These structures correlate in size with the α-synuclein$_{A30P}$-positive aggregates shown in Fig. 2*D* and could as above be instigated by bafilomycin A1 treatment of control cells alone (Fig. 6, *E* and *H*).

Co-expression of p25α Causes Unconventional Secretion of α-Synuclein by Exophagy—Despite the ability of p25α to impair autophagosome maturation and autolysosomal degradation, p25α expression surprisingly correlated with an augmented clearance of α-synuclein (Fig. 7*A*). In addition, clearance of α-synuclein in PC12 cells without p25α was not completely suppressed by addition of leupeptin/pepstatin A, which inhibits endosomal and lysosomal degradation. We therefore tested if α-synuclein was secreted to the surroundings by the PC12 cells. The conditioned medium after 2 days of transgene expression was precipitated with TCA and then analyzed for presence of α-synuclein by Western blotting. When expressed alone, both α-synuclein$_{wt}$ and to a higher extent α-synuclein$_{A30P}$ was secreted into the medium; however, secretion of α-synuclein was greatly up-regulated by p25α co-expression (Fig. 7*B*). TPPP/p25α was also secreted (Fig. 7*B*), it but had a longer cellular half-life than α-synuclein (data not shown).

In yeast, exocytosis of autophagosomes constitutes an unconventional secretion pathway (37). Consistent with this and our observations above, addition of the autophagy inhibitor 3-MA, which inhibits class III PI3K activity required for formation of the isolation membrane, significantly reduced secretion of α-synuclein in PC12 cells co-expressing α-synuclein$_{A30P}$ and p25α (Fig. 7, *B* and *F*). Autophagy was effectively inhibited at the concentrations of 3-MA used, as the drug caused p62/SQSTM1 accumulation (Fig. 7*B*) (15, 20). In cells only expressing α-synuclein$_{A30P}$, 3-MA on the contrary induced an increase in secretion of α-synuclein (Fig. 7, *B* and *F*). This is likely due to the persistent inhibitory effect of 3-MA on class I PI3K (which normally activates the mTOR pathway, and thereby opposes autophagy) and a transient inhibition of class III PI3K (required in both mTOR-dependent and -independent autophagy) as reported previously (38).

For space considerations, Western blots of conditioned medium have generally been cropped to show only monomer α-synuclein, but Fig. 7*C* shows that SDS-insoluble oligomeric and high molecular weight α-synuclein immunoreactive species were secreted alongside monomers and correlated in intensity with each other. By densitometry of Western blots, we estimate that between 6 and 12% of the total cellular α-synuclein$_{A30P}$ was present in the medium after 2 days of culture. This makes it difficult to see changes in cellular levels of α-synuclein by Western blotting, but p25α expression markedly lowered the levels of endogenous α-synuclein in cell lysates, and this correlated with secretion of α-synuclein into the medium (Fig. 7*D*). The low amounts of secreted endogenous α-synuclein in the medium could only be detected by immunoprecipitation and not by TCA precipitation.

TPPP/p25α-induced secretion of α-synuclein was not a consequence of the inability of p25α-expressing cells to form an extensive neurite network (see Fig. 1, *A* and *B*). If PC12 cells were fully differentiated with NGF for 4–6 days before induction of p25α expression with doxycycline, there was no subsequent effect on the neuritic network, and the cells maintained an augmented secretion of α-synuclein 4.9 ± 1.3 (n = 3)-fold higher than control cells without p25α (data not shown). Secretion was however a function of NGF differentiation, as the amount of α-synuclein secreted from undifferentiated PC12 cells (with or without p25α expression) was less than 25% that of differentiated cells (data not shown).

Chemical or Genetic Modification of the Autophagosomal-Lysosomal Pathway Affects Secretion of α-Synuclein—We further tested the effects of chemical modulation of the autophagosomal-lysosomal pathway on the secretion of α-synuclein by using a panel of inhibitors or enhancers of different forms of autophagy. As seen in Fig. 7, *E* and *F*, inhibition of lysosomal function by either leupeptin/pepstatin A or even more promi-

FIGURE 3. **Autophagy markers LC3B and p62/SQSTM1 co-localize with α-synuclein.** Indirect immunofluorescence of PC12 cells expressing α-synuclein$_{A30P}$ alone (α-SNC$_{A30P}$) (*A*) or together with p25α (*B* and *C*) to visualize α-SNC (mAb LB509) distribution in relation to LC3B (*A* and *B*) or p62/SQSTM1 (*C*). Co-localization between α-SNC and the respective markers are indicated with *arrows*. *Bars, A–C,* 10 μm in the *left panels* and 5 μm in close-ups. PC12-α-SNC$_{A30P}$ (*D–F*) or PC12-α-SNC$_{A30P}$/p25α (*G–I*) cells expressing mCherry-eGFP-LC3B were fixed and processed for cryo-immunogold labeling with mouse monoclonal anti-α-SNC (mAb LB509) antibodies and rabbit polyclonal anti-GFP antibodies, followed by secondary 14- or 7-nm gold-conjugated anti-mouse or anti-rabbit antibodies, respectively. *E,* micrograph shows several autophagosomes containing only labeling for eGFP-LC3B (*black open arrows*) and a single autophagosome containing both α-SNC and eGFP-LC3B (*black filled arrow*), which is also true of an electron dense autolysosome (*open white arrow*). The *closed white arrow* points to a cytosolic inclusion staining for both α-SNC and eGFP-LC3B. *D,* autolysosome with both labels is also shown at higher magnification. *F,* nascent autophagosome with both labels (*black open arrow*) and a vacuole/autophagosome containing only aggregated label for α-SNC (*black filled arrow*). In PC12 cells co-expressing α-SNC$_{A30P}$ and p25α (*G–I*), the number of autophagosomes was increased and recently formed autophagosomes (*open black arrows*) and amphisomes (*white open arrows*), including lamellar bodies (*white, open arrow* in *G*) and electron dense late autophagosomal elements (*white, open arrows* in *H*) contained label for both α-SNC and eGFP-LC3B. *White closed arrow* in *G* points to a late endosome devoid of immunoreactivity for either α-SNC or eGFP-LC3B, and the *small white arrow* in *H* points to extracellular α-SNC immunoreactivity associated with microvilli (*MV*) on the cell surface (*white arrowheads*). *I,* electron dense late autophagosomal element from *H* shown at higher magnification. *M,* mitochondria. *Bars, D–H*, 500 nm.

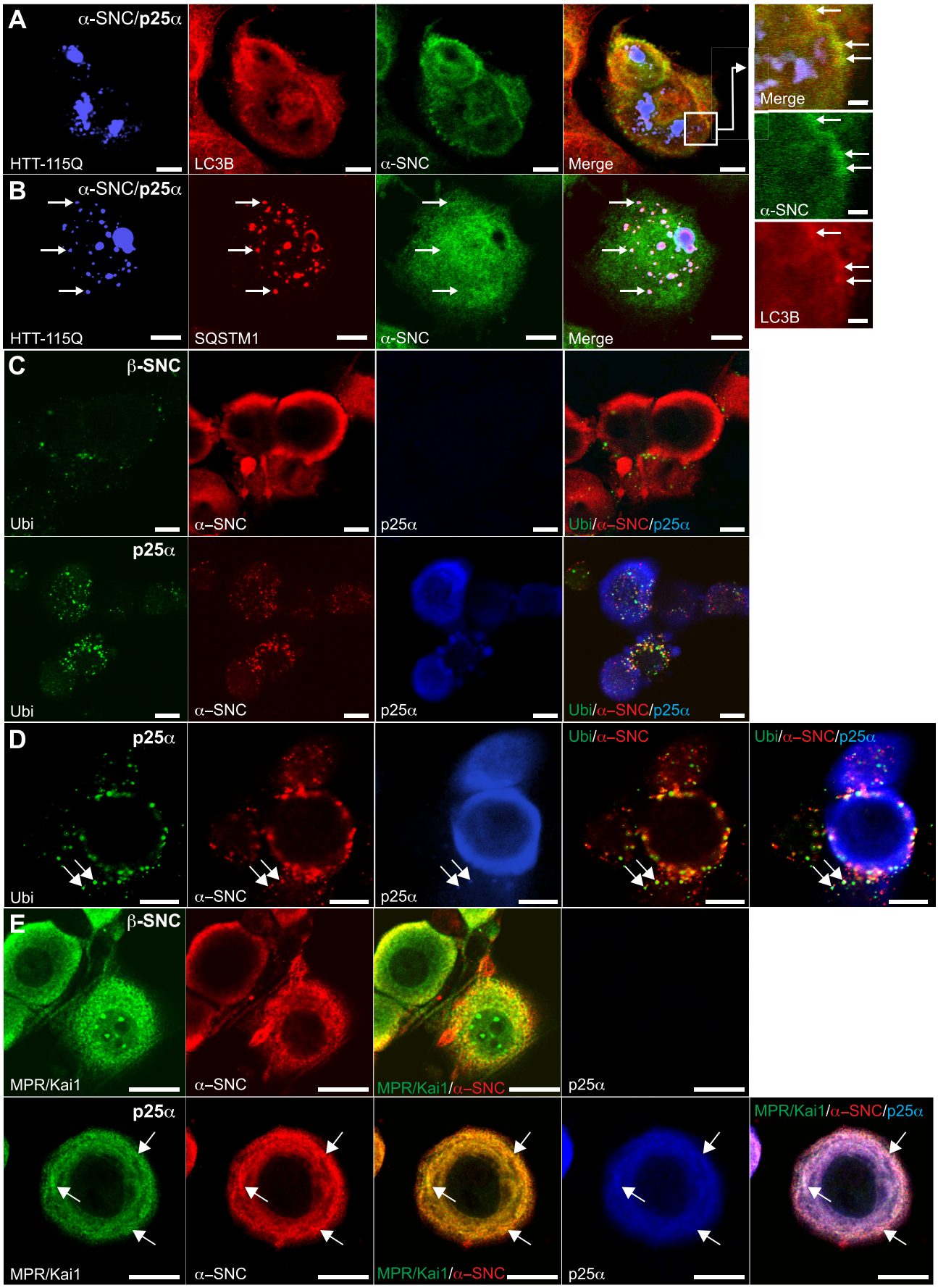
A
α-SNC/p25α
HTT-115Q
LC3B
α-SNC
Merge
Merge
α-SNC
LC3B
B
α-SNC/p25α
HTT-115Q
SQSTM1
α-SNC
Merge
C
β-SNC
Ubi
α–SNC
p25α
Ubi/α–SNC/p25α
p25α
Ubi
α–SNC
p25α
Ubi/α–SNC/p25α
D
p25α
Ubi
α–SNC
p25α
Ubi/α–SNC
Ubi/α–SNC/p25α
E
β-SNC
MPR/Kai1
α–SNC
MPR/Kai1/α–SNC
p25α
p25α
MPR/Kai1
α–SNC
MPR/Kai1/α–SNC
p25α
MPR/Kai1/α–SNC/p25α

nently with bafilomycin A1, which mimics the p25α-induced block of autophagosomal fusion with lysosomes, caused a clear up-regulation of α-synuclein secretion. This was also the case when PC12 cells with or without p25α expression were treated with trehalose, an mTOR-independent enhancer of autophagy (39), which correlated with marked increases in LC3B-II levels (Fig. 7*E*). The increase in LC3B-II levels caused by bafilomycin and leupeptin/pepstatin is directly due to suppression of degradation of conjugated LC3B-II in lysosomes, whereas the increase mediated by trehalose is due mainly to increased conversion of LC3B. In contrast, rapamycin, an enhancer of mTOR-dependent autophagy (starvation-induced autophagy), did induce transient conversion of LC3B (see below), but only increased secretion moderately in PC12-α-synuclein$_{A30P}$ cells and not at all in p25α-expressing cells. Trichostatin, which inhibits HDAC6 and thereby deacetylation of cortactin required for fusion of QC autophagosomes with lysosomes (40), caused a modest up-regulation of α-synuclein secretion in PC12 cells with or without p25α expression.

The involvement of autophagosomes in secretion was verified by shRNA knockdown of ATG5, which is required for elongation and formation of the autophagosomal isolation membrane (12). Using a combination of two different shRNA constructs, ATG5 protein expression in PC12-α-synuclein$_{A30P}$/p25α cells was reduced to 30%, which correlated with a decreased conversion of LC3B-I to LC3B-II and a 60% reduction in the amount of α-synuclein secreted (Fig. 7, *G–I*). Collectively, the data demonstrate that p25α mediates unconventional secretion of α-synuclein through a pathway, which is dependent on autophagosome formation. In contrast, the levels of Htt-115Q-GFP detected in the conditioned medium of PC12 cell lines co-expressing huntingtin constructs were low and did not change significantly upon p25α expression (Fig. 7, *J* and *K*), likely reflecting the aggresome inclusion of Htt-115Q-GFP noted previously (Fig. 4, *A* and *B*).

Trehalose and Rapamycin-induced Autophagosomes Are Differentially Affected by p25α Expression—The different effects of trehalose and rapamycin on LC3B conversion and α-synuclein secretion after 48 h made us examine more carefully the effect of these autophagy enhancers. Fig. 8*A* shows the typical distribution and fluorescence of the mCherry-eGFP-LC3B construct in untreated PC12-α-synuclein/p25α cells. As expected, 3-MA caused the number of autophagosomes to decrease, and apart from a few large vacuoles LC3B was mainly cytosolic. Trehalose induced an increased number of LC3B-positive structures, but as in the control situation, the autophagosomes were inhibited in their maturation (both red and green fluorescence). In contrast, the effect of rapamycin on LC3B conversion was transient (<24 h) and did not differ significantly from untreated cells after 48 h (Figs. 7, *E* and *F,* and 8, *E* and *F*). However, maturation of rapamycin-induced autophagosomes in terms of acidification progressed unimpeded by p25α expression as assessed by the mCherry-eGFP-LC3B construct, which displayed an increased number of vesicular profiles with only red fluorescence (Fig. 8*D*). Collectively, the data therefore indicate that p25α expression specifically affects selective mTOR-independent autophagy.

Secretion of α-Synuclein Depends on Exocytosis of a Compartment with Late Endosomal/Amphisomal Characteristics—Exocytosis of late endosomal elements, including amphisomes, which arise from fusion with late endosomes, causes insertion of phosphatidylserine into the exoplasmic leaflet of the plasma membrane, and this can be detected by annexin-V staining (41). As binding of annexin-V to the cell surface is also used for detection of apoptosis, we co-stained the cells with anti-caspase-3 antibodies to separate the two phenomena. As shown in Fig. 9, *A* and *B*, binding of Alexa-conjugated annexin-V to the cell surface was ~3-fold increased up to 45% by the expression of p25α, while at this time point (2 days of transgene expression) apoptosis detected by immunoreactivity for cleaved caspase-3 did not exceed 4% (Fig. 9*A*, see also Fig. 1*E*) indicating exocytosis of late endosomes and amphisomes. Exocytosis of late endosomes causes the release of small intraluminal vesicles, termed exosomes, to the extracellular medium (42), and it has recently been forwarded that α-synuclein can be taken up directly into late endosomes and secreted with exosomes (43). As shown in Fig. 9*C*, PC12-α-synuclein$_{A30P}$/p25α cells expectedly secreted a higher amount of exosomes (identified by flotillin-1 expression) into the medium than α-synuclein$_{A30P}$-expressing PC12 cells. However, almost all the secreted monomeric or high molecular weight α-synuclein was soluble and did not associate with the exosome fraction, which we estimate contained less than 3% of the total secreted α-synuclein. It has recently been shown that the small GTPase Rab27A is essential for exocytosis of late endosomes by promoting the fusion of late endosomes with the plasma membrane (44). When we either silenced Rab27A by shRNA or expressed Rab27A mutants in PC12-α-synuclein$_{A30P}$/p25α cells, we encountered an increased mortality, which precluded analysis of active secretion of α-synuclein. However, in PC12 cells expressing α-synuclein$_{A30P}$ alone, expression of dominant active (Q78L) or negative (T23N) mutants of Rab27A increased or decreased secretion of α-synuclein, respectively, despite a quite low efficiency of transduction with this pLenti vector (~40% transduced cells for Rab27A-Q78L and 25% for Rab27A-T23N) (Fig. 9, *D–F*).

HDAC6 Deacetylase Activity Is Decreased by p25α Expression and HDAC6 shRNA Knockdown Promotes α-Synuclein Secretion—HDAC6 is the major cytosolic deacetylase in neurons and is required for QC autophagosome maturation at the

FIGURE 4. **TPPP/p25α-induced autophagy is selective and also affects endogenous rat α-synuclein.** *A* and *B,* PC12 α-synuclein$_{A30P}$/p25α (α-SNC$_{A30P}$/p25α) cells were transduced with lentivector pHR-cPPT.CMV.W-Htt-115Q-GFP, and after 2 days α-SNC and p25α expression was induced with doxycycline for a further 2 days. Cells were then fixed and processed for indirect immunofluorescence to visualize the following: *A,* Htt-115Q-GFP (*blue*), LC3B (*red*), and α-SNC (*green*; BD Transduction Laboratories), or *B,* Htt-115Q-GFP (*blue*), p62/SQSTM1 (*red*), and α-SNC (*green*; BD Transduction Laboratories). The *box* in *A* is shown at higher magnification to the *right*. Note that α-SNC preferentially co-localizes with LC3B, whereas Htt-115Q-GFP co-localizes with p62/SQSTM1. *Bars,* 10 μm and in *right panels* 2 μm. *C,* NGF-differentiated PC12 cells expressing either β-synuclein (*β-SNC*) as control or p25α were analyzed by indirect immunofluorescence to localize polyubiquitin, endogenous α-SNC (Abcam mAb EP1646Y), and p25α as indicated. *D,* PC12 cells expressing p25α and stained as above at higher magnification. *Arrows* indicate co-localization of α-SNC with ubiquitin and p25α. *E,* control (*β-SNC*) or p25α-expressing PC12 cells were processed for indirect immunofluorescence with rat anti-p25α mAb, mouse anti-α-SNC mAb LB509, and rabbit polyclonal antibodies against KAI1 and MPR. *Arrows* indicate vesicular structures with co-localization of α-SNC and KAI1/MPR, which to a certain extent also co-localize with p25α. *Bars, C–E*, 10 μm.

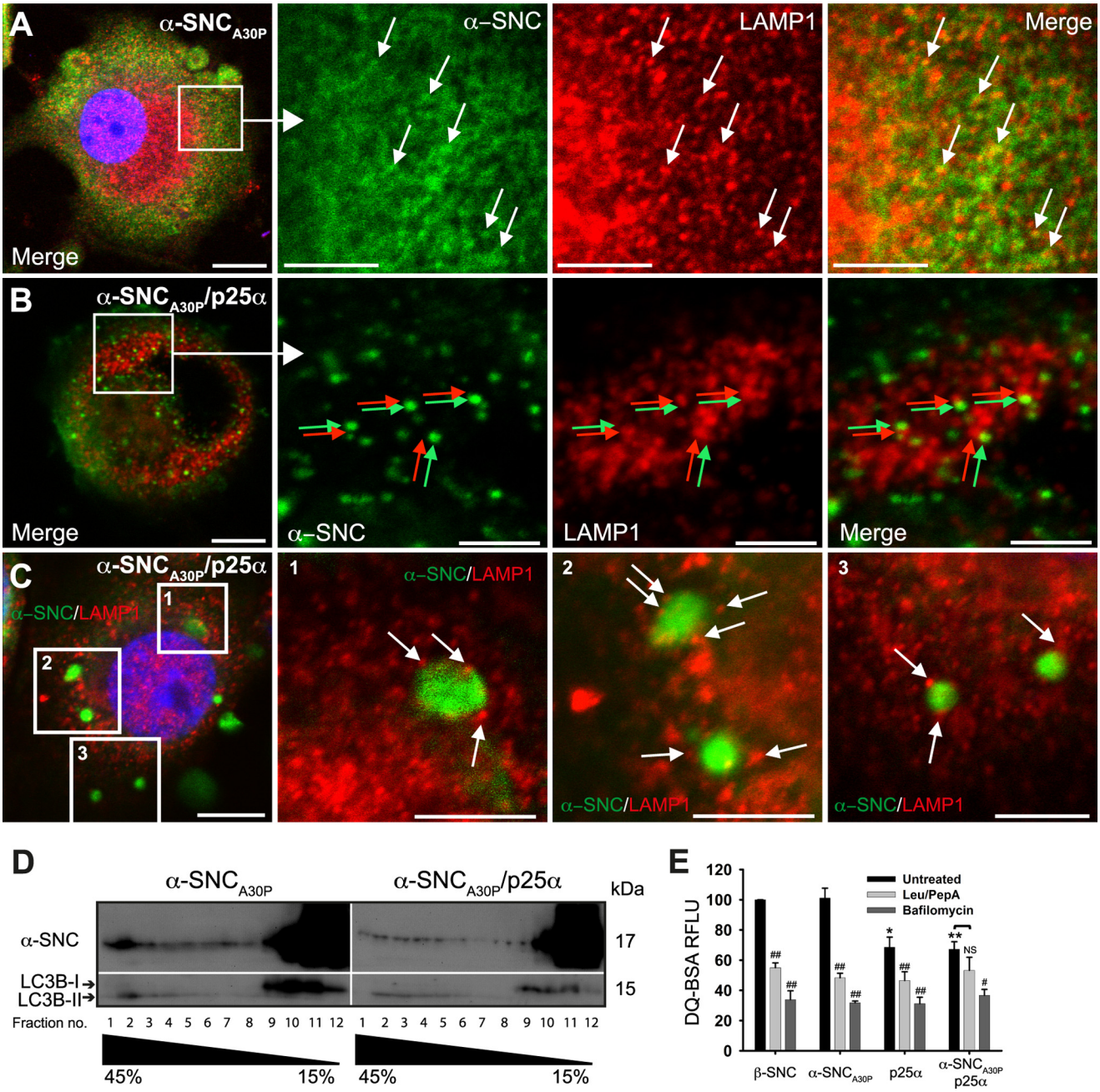

FIGURE 5. **Expression of p25α prevents α-synuclein in reaching lysosomes.** *A–C,* indirect immunofluorescence of leupeptin/pepstatin A-treated PC12 cells expressing α-synuclein$_{A30P}$ (α-SNC$_{A30P}$) alone (*A*) or together with p25α (*B* and *C*), showing the distribution of α-SNC$_{A30P}$ (Abcam LB509) and the lysosomal marker LAMP1. *Arrows* in *A* indicates co-localization between the antigens, and *arrows* in *B* (*red* and *green*) and *C* (*white*) indicate that, although closely apposed, α-SNC immunoreactivity is distinct from that of LAMP1. *Bars, A–C,* 10 μm in the *left panels* and 5 μm in *close ups*. *D,* homogenates from PC12 cells expressing α-SNC$_{A30P}$ or α-SNC$_{A30P}$/p25α were fractionated on a 15–45% sucrose gradient and aliquots of collected fractions analyzed by Western blotting of α-SNC (BD Transduction Laboratories) and LC3B. The blots are representative of two independent experiments. Note that p25α decreases the amount of α-SNC present in heavy fractions 1–3, which also contains exclusively autophagosome-associated LC3B-II. *E,* flow cytometric analysis of PC12 cells incubated with DQ-BSA for 6.5 h with or without either bafilomycin A1 (100 nM) or leupeptin (50 μg/ml)/pepstatin A (67 μg/ml) treatment. DQ-BSA fluorescence intensity was normalized to β-synuclein (*β-SNC*)-expressing PC12 cells, and the *bar graph* shows mean ± S.E. of relative fluorescence units (*RFLU*) ($n = 3$). * denotes a statistic significant decrease in relative fluorescence units for untreated cell lines when compared with untreated β-SNC-expressing cells; # denotes statistic significant decrease within the same cell line after chemical treatment; *NS,* nonsignificant.

level of lysosome fusion (40). It has recently been demonstrated that p25α inhibits the deacetylase activity of HDAC6 (27). In accordance with this, the level of acetylated tubulin, a substrate of HDAC6, was increased by p25α expression in PC12 cells (Fig. 10*A*), which could critically influence transport of mature organelles or autophagosome formation. As shown above, chemical inhibition of HDAC6 with trichostatin A increased secretion of α-synuclein (Fig. 7, *E* and *F*), so we started out by substantiating this correlation further by silencing HDAC6 with shRNA in PC12 cells only expressing α-synuclein$_{A30P}$ to mimic the p25α-induced inhibition of HDAC6. Fig. 10, *B* and *C,* shows that expression of HDAC6-specific shRNA increased the level of acetylated tubulin more than 2-fold in PC12-α-synuclein$_{A30P}$ cells without altering the total pool of α-tubulin.

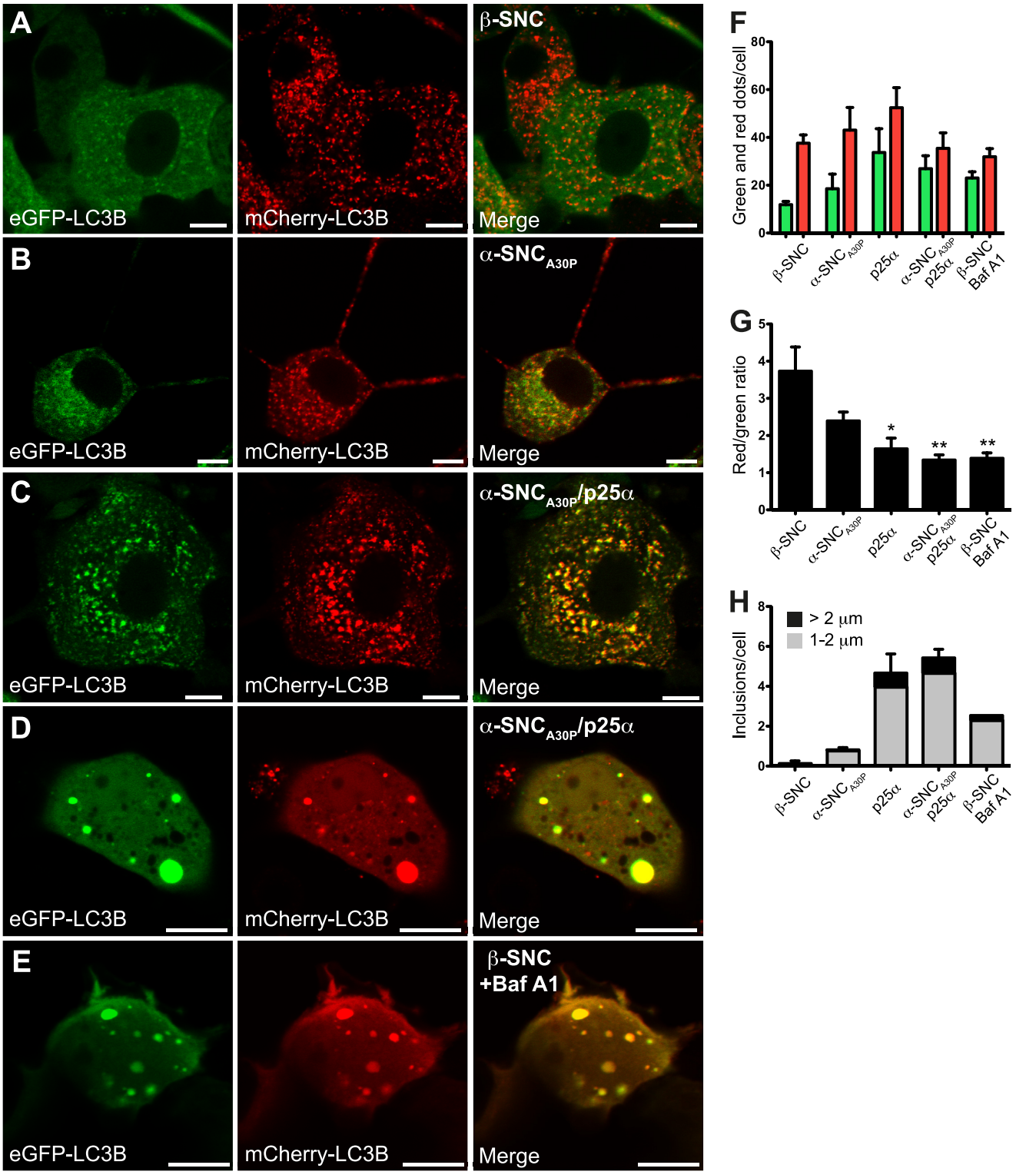

FIGURE 6. **Expression of p25α impairs the autophagosomal flux.** *A–E*, confocal microscopy images of live PC12 cells co-expressing mCherry-eGFP-LC3B with either β-synuclein (β-SNC) (*A*), α-SNC$_{A30P}$ (*B*), α-SNC$_{A30P}$/p25α (*C* and *D*), or β-SNC-expressing PC12 (*E*) cells treated with 20 nM bafilomycin A1 (*Baf A1*) for 6 h. *Bars*, 10 μm. *F*, *bar graph* shows absolute mean ± S.E. of mCherry (*red*) and eGFP (*green*) fluorescent structures per cell profile of three independent experiments. In each experiment 25–30 cells from each cell line were analyzed. *G*, same data as *F* presented as the ratio between the absolute numbers of mCherry and eGFP fluorescent dots. *H*, mCherry- and eGFP-positive structures larger than 1 μm in diameter were quantified according to size (1–2 μm: *gray*; >2 μm: *black*). The *bar graph* shows the number of inclusions per cell and represents mean ± S.E. of three independent experiments.

Although this was a modest increase in acetylated tubulin levels compared with α-synuclein$_{A30P}$/p25α-expressing PC12, it translated into a disproportionally large increase in secreted α-synuclein (Fig. 10, *B* and *D*), probably reflecting that HDAC6 alters transport as well as fusion of autophagosomes with lysosomes. We further tested the effect of HDAC6 inhibition on

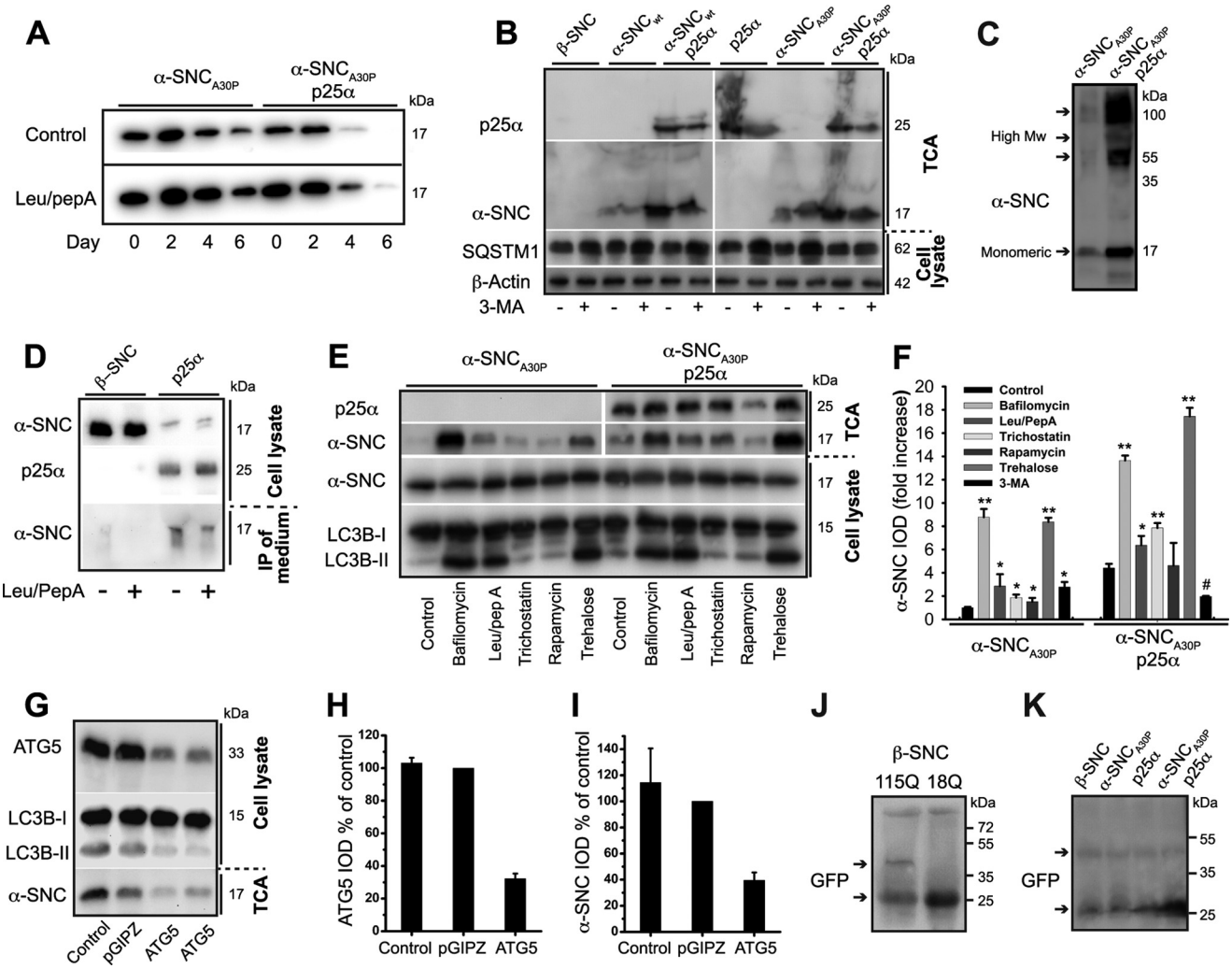

FIGURE 7. **TPPP/p25α induces α-synuclein secretion, which can be modified by regulators of the autophagosomal degradation pathway.** *A,* PC12 cells expressing α-synuclein$_{A30P}$ alone (*α-SNC$_{A30P}$*) or with p25α (*α-SNC$_{A30P}$/p25α*) were predifferentiated with NGF for 2 days and transgene expression induced for additionally 2 days. Doxycycline was then withdrawn, and the cells chased for 6 days with or without leupeptin (50 μg/ml) and pepstatin A (67 μg/ml). Representative Western blots using anti-α-SNC (BD Transduction Laboratories) shows clearance of α-SNC from cell lysates acquired from day 0, 2, 4, and 6 after doxycycline withdrawal. *B,* representative Western blots using anti-α-SNC (BD Transduction Laboratories), p62/SQSTM1 (*SQSTM1*), and β-actin of cell lysates and TCA-precipitated conditioned media obtained from PC12 cell lines expressing β-SNC, α-SNC wild type (*α-SNC$_{wt}$*), or α-SNC$_{A30P}$ with or without p25α in the presence or absence of 3-MA (10 mM) ($n = 3$). *C,* representative Western blot of TCA-precipitated medium obtained from PC12 cells expressing α-SNC$_{A30P}$ alone or together with p25α using mouse anti-α-SNC (BD Transduction Laboratories). Notice the presence of both monomeric (17 kDa) and high molecular weight (*High Mw*) forms of secreted α-SNC. *D,* PC12 cells expressing β-SNC (as control) or p25α were treated or not with leupeptin/pepstatin A (50 and 67 μg/ml) for the last 24 h of culture before analysis of endogenous α-SNC in cell lysates and immunoprecipitates from conditioned medium (using BD Transduction Laboratories and LB509 mAbs) by Western blotting (using anti-α-SNC rabbit mAb EP1646Y) as indicated. Data are representative of three independent experiments. *E,* PC12 cells expressing α-SNC$_{A30P}$ or α-SNC$_{A30P}$/p25α were treated with bafilomycin A1 (15 nM), leupeptin (50 μg/ml)/pepstatin A (67 μg/ml), trichostatin A (20 μM), rapamycin (0.5 μM), trehalose (100 mM), or left untreated (*control*) for 48 h concurrently with doxycycline induction before Western blot analysis of TCA-precipitated conditioned media and cell lysates using antibodies as indicated. *F, bar graph* shows fold increase in integrated optical density (*IOD*) of TCA Western blot bands of secreted α-SNC (BD Transduction Laboratories) obtained from *B* and *E* relative to untreated PC12-α-SNC$_{A30P}$ cells. Mean ± S.E. of three independent experiments are shown. *G,* TCA-precipitated conditioned medium or cell lysates from PC12-α-SNC$_{A30P}$/p25α cells with or without stable co-expression of either control (*pGIPZ*) or ATG5 shRNA were analyzed by Western blotting using anti-α-SNC (BD Transduction Laboratories), ATG5, or LC3B antibodies as indicated. *H, bar graph* shows IOD of ATG5 western bands normalized to PC12 cells expressing control shRNA (*pGIPZ*) and represents mean ± S.E. of three independent experiments. *I, bar graph* shows IOD of α-SNC western bands (TCA samples) normalized to PC12 cells expressing control shRNA (*pGIPZ*) and represents mean ± S.E. of three independent experiments. *J* and *K,* PC12 cell populations as indicated were transduced with either Htt-18Q-GFP or Htt-115Q-GFP for 2 days before transgene induction for a further 2 days. Conditioned medium was then TCA-precipitated and analyzed by Western blotting with polyclonal rabbit anti-GFP antibodies. *J,* a ~50-kDa band (*upper arrow*) immunoreactive with anti-GFP antibodies is seen exclusively in the conditioned medium from HTT-115Q-GFP-expressing cells but not from control HTT-18Q-GFP cells. *K,* similar secretion of HTT-115Q-GFP was observed in PC12 cells expressing β-SNC, p25α, or α-SNC$_{A30P}$ with or without p25α expression. The increased reactivity to monomer GFP to the *right* on the blot is caused by overflow from an adjacent (data not shown) cell lysate lane. *Upper* and *lower arrows* indicate HTT-115Q-GFP fusion protein and monomeric GFP, respectively.

autophagosomal maturation by flow cytometric analysis of the pH-sensitive eGFP moiety of the mCherry-eGFP-LC3B construct, which was expressed at equal levels in the PC12 cell populations (Fig. 10*E*). As expected, expression of p25α increased eGFP fluorescence in the cells due to inhibited maturation and acidification, and this effect was replicated in PC12 cells either expressing β-synuclein or α-synuclein$_{A30P}$ by treatment with trichostatin (Fig. 10*F*).

During live cell imaging of the mCherry-eGFP-LC3B construct, we noticed that the mobility of autophagosomes

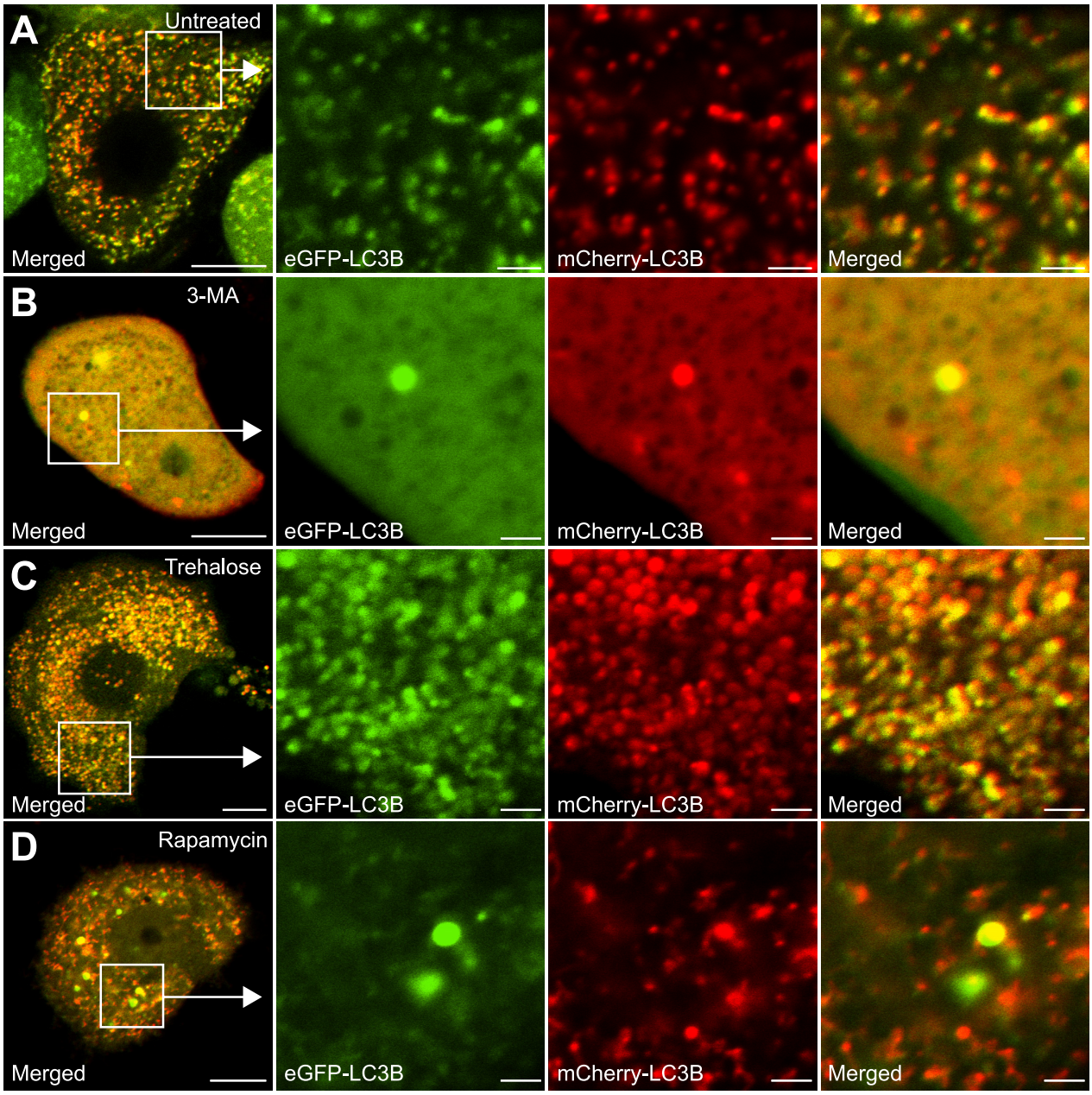

FIGURE 8. **mTOR-dependent and -independent autophagy enhancers rapamycin and trehalose, respectively, differentially affect the distribution and fluorescence properties of mCherry-eGFP-LC3B.** *A–D*, PC12-α-synuclein$_{A30P}$/p25α (α-*SNC*$_{A30P}$/p25α) cells expressing mCherry-eGFP-LC3B were treated with 3-MA (10 mM), trehalose (100 mM), or rapamycin (0.5 μM) as indicated, for the last 48 h of culture, before live imaging with a Zeiss LSM510 confocal microscope. Note that 3-MA causes the diffusive cytoplasmic distribution of the mCherry-eGFP-LC3B construct, whereas trehalose induces the massive accumulation of large autophagosomal vacuoles that emit both mCherry and GFP fluorescence. In contrast, autophagy induced by rapamycin increased the proportion of autophagosomal vacuoles with predominant emission of only mCherry-fluorescence indicating correct acidification. *Bars,* 10 μm, *enlarged images* 2 μm. The images shown are representative of three independent experiments. *E*, PC12-α-SNC/p25α cells were treated with 0.5 or 1 μM rapamycin for different time intervals as indicated, and cell lysates were then analyzed by Western blotting for conversion of LC3B and levels of β-actin (loading control). Samples from the 48-h time point were run on separate gel due to lack of wells. The Western blot is representative of two independent experiments. *F*, integrated optical density (*IOD*) of LC3B-II bands from the experiment shown in *E* were normalized to levels of β-actin and plotted over time.

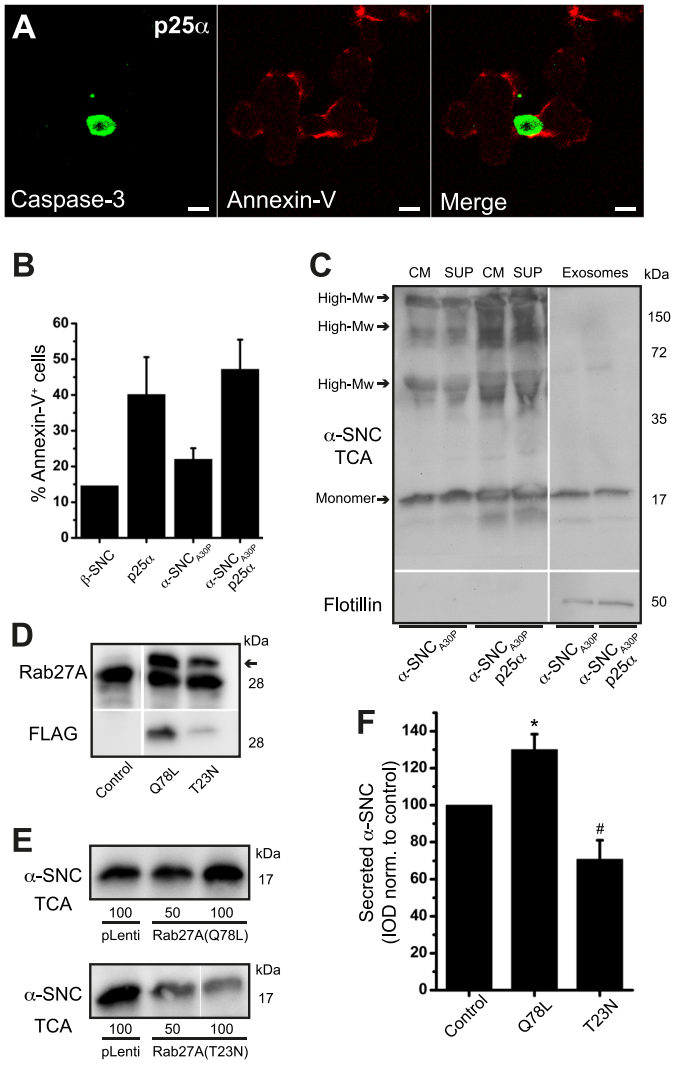

FIGURE 9. **Secretion of α-synuclein is mediated by compartments with late endosomal/amphisomal characteristics.** *A,* p25α-expressing PC12 cells were incubated with Alexa 568-conjugated annexin-V on ice before fixation and indirect immunofluorescence with antibodies against cleaved caspase-3. Note widespread annexin-V surface staining in the absence of caspase-3 immunoreactivity. *Bar,* 10 μm. *B,* PC12 cell lines labeled with Alexa 488-conjugated annexin-V on ice were analyzed by flow cytometry. The *bar graph* shows percentage annexin-V positive cells of the whole cell population and represents mean ± S.E. of three independent experiments. *C,* conditioned medium (*CM*) from PC12 cells expressing α-synuclein$_{A30P}$ (*α-SNC$_{A30P}$*) with or without p25α was centrifuged at 100,000 × *g* to obtain a pellet (containing exosomes) and a supernatant (*sup*). Aliquots were then Western blotted with anti-α-SNC (BD Transduction Laboratories) or anti-flotillin-1 (exosome marker) antibodies. The exosome fraction was applied on the gel at 6-fold the relative load of supernatant and medium. The blot is representative of two independent experiments. *D–F,* PC12-α-SNC$_{A30P}$ cells were differentiated for 2 days and transduced at two different multiplicities of infection with lentivectors constitutively expressing FLAG-tagged Rab27A-Q78L (dominant positive) or Rab27A-T23N (dominant negative). Control wells received a GFP-expressing vector (*pLenti*). *D,* after 2 days of transgene induction cell lysates were prepared to show expression of Rab27A using anti-Rab27A mAb 4B12 (*arrow* points to transgene) or anti-FLAG antibodies. *E,* conditioned medium was TCA-precipitated and Western blotted with anti-α-SNC antibodies (BD Transduction Laboratories). *F, bar graph* shows mean ± S.E. of the integrated optical density (*IOD*) of α-SNC Western blot bands normalized to control-transduced cells ($n = 3$). * and # denotes a statistic significant increase or decrease, respectively, in α-SNC secretion when compared with control-transduced PC12 cells.

appeared severely reduced in p25α-expressing cells, and to quantitate this, we applied FRAP on PC12 cells constitutively expressing the mCherry-eGFP-LC3B construct. The percentage of recovered mCherry fluorescence after bleaching in small regions of interest is shown in Fig. 10, *G–I*, where it is evident that p25α expression suppressed recovery with 80%. Although co-expression of α-synuclein depressed recovery further, α-synuclein alone had no effect. Inhibition of cytosolic deacetylase activity with either trichostatin or HDAC6 shRNA in α-synuclein$_{A30P}$-expressing control cells replicated the effect of p25α expression (Fig. 10*I*). The less efficient reduction in autophagosome mobility after HDAC6 knockdown when compared with trichostatin treatment could be due to inefficient transduction as the knocked down cells could not be identified before selecting cells for FRAP analysis. See the supplemental movie of autophagosome mobility in the β-synuclein- and α-synuclein$_{A30P}$/p25α-expressing PC12 cells from Fig. 10, *G* and *H*.

Rab GTPases Modulate α-Synuclein Secretion and Toxicity—The Rab family of small GTPases are important regulators of vesicular transport and fusion events along the biosynthetic and endosomal pathway. Recent genetic screens in yeast and further experimentation in animal models showed that Rab1A and Rab8 alleviate α-synuclein-induced cytotoxicity (45–47). We therefore overexpressed Rab1A and Rab8 in PC12 cells to observe the effect on α-synuclein secretion (Fig. 11*A*). Additionally, we expressed a Rab7-GFP fusion protein, as this GTPase is associated with maturation of late endosomal compartments by regulating fusion with lysosomes (48, 49). Rab3A is known to regulate exocytosis of chromaffin-containing vesicles in PC12 cells and was used as a control. Although expression of Rab1A increased secretion of α-synuclein$_{A30P}$ 2-fold in PC12 cells only expressing α-synuclein$_{A30P}$, it had no significant effect in PC12 cells co-expressing p25α (Fig. 11, *B* and *C*). However, most markedly, Rab8 increased α-synuclein$_{A30P}$ secretion severalfold in both cell lines without altering LC3B conversion significantly. To our surprise, expression of Rab7-GFP, which we expected to promote autophagosome maturation and lessen secretion, also modestly increased secretion. Interestingly, while promoting secretion, expression of Rab7 or Rab8 both reduced cytotoxicity of α-synuclein and p25α expression (Fig. 11, *H* and *I*), underscoring that within the time frame of analysis used throughout the study, release of α-synuclein is an active process and not correlated with cell death. When we analyzed the effect of Rab expression on the distribution of α-synuclein by confocal microscopy, we observed that neither Rab3 (data not shown) nor Rab1A affected the distribution of α-synuclein$_{A30P}$ (compare Figs. 11*D* with 2*C*).

In contrast, Rab8, which was mainly localized to subcortical areas of the cytosol, caused a more peripheral distribution of α-synuclein$_{A30P}$ (Fig. 11*E*). Rab8 could be seen to coat peripheral membrane elements also positive for LC3B as shown in Fig. 11*F*, identifying them as autophagosomes/amphisomes. Interestingly, Rab8 consistently and specifically (compared with Rab3 as control) caused accumulation of particular material on the cell surface or substratum, which was immunoreactive with anti-KAI1 antibodies. A fraction of this material was also positive for α-synuclein, and it likely represents the secreted and aggregated luminal contents of amphisomes and late endosomes (Fig. 11*G*).

DISCUSSION

The aim of this study was to evaluate the role of autophagy in degradation and unconventional secretion of α-synuclein species from dopaminergic-like neurons in culture.

TPPP/p25α Impairs the Autophagosomal Degradation Pathway—Aggregated or modified forms of α-synuclein are substrates of all major degradative systems *in vivo* and *in vitro*, including the ubiquitin proteasome system, chaperone-mediated autophagy, and macroautophagy (8, 9, 50, 51). In this study we have used p25α expression as a tool to increase aggregation and autophagosomal uptake of α-synuclein. However, p25α is also in its own right an interesting protein in the context of α-synucleinopathy, because p25α is ectopically expressed in dopaminergic neurons in PD, and it is a component of Lewy bodies purified from post-mortem brain of patients with PD (24). Upon prolonged culture p25α-expressing cells eventually

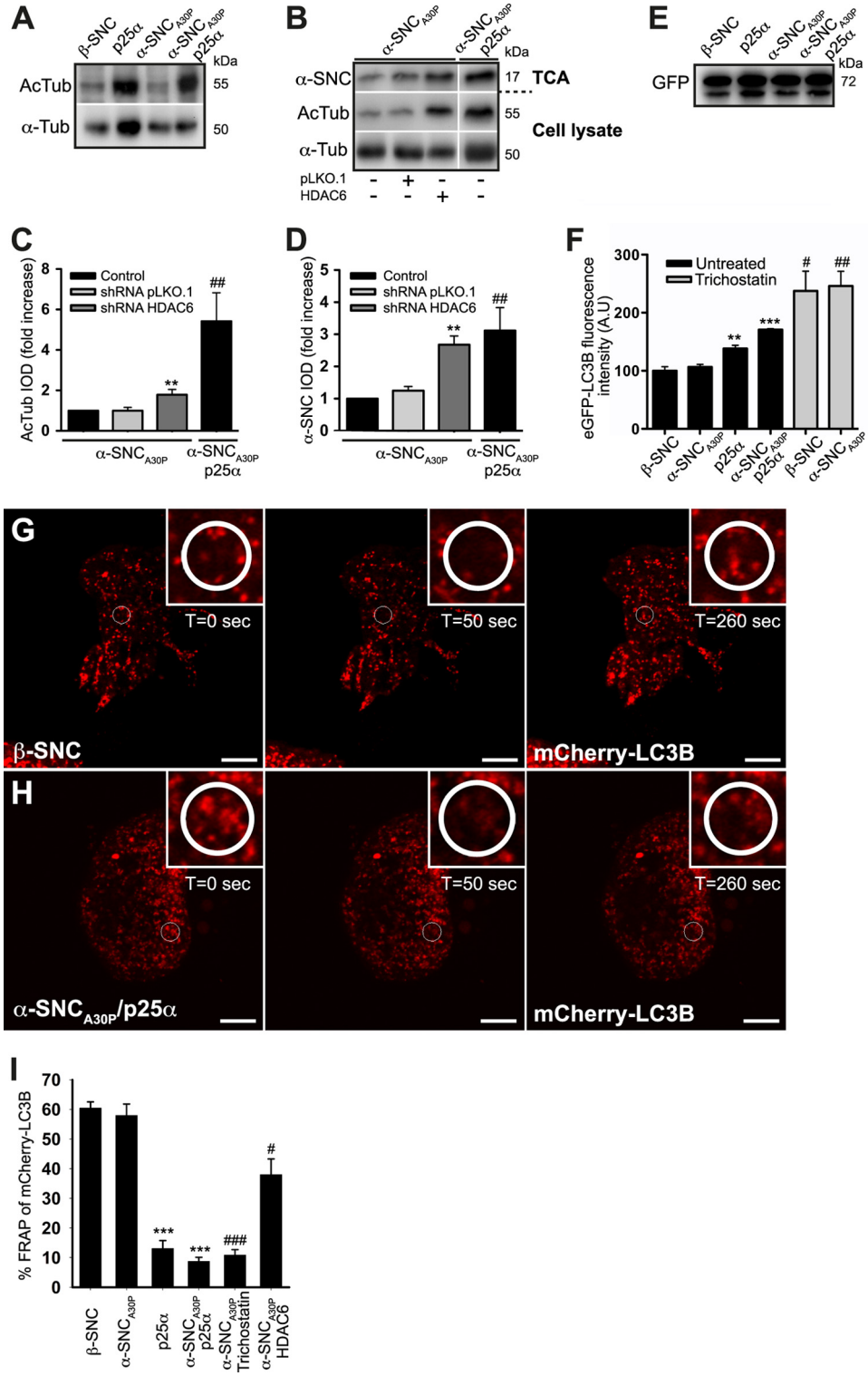

succumb to apoptotic cell death. However, within the time frame of experimentation used here, α-synuclein or p25α expression only raised mortality associated with neuronal differentiation by a few percent (from 15% in NGF-differentiated control cells to 18% in α-synuclein/p25α-expressing cells).

It has recently been shown that p25α inhibits the deacetylase activity of HDAC6 (27), which is the predominant deacetylase in the cytosol of neurons, and in accordance with this, p25α expression in PC12 cells increased tubulin acetylation about 6-fold. Expression of HDAC6 shRNA in the absence of p25α afforded a 2-fold increase in levels of acetylated tubulin, but this still correlated with a slowed maturation of autophagosomes and a 3-fold increase in levels of secreted α-synuclein, suggesting that these effects of p25α expression are a consequence of HDAC6 inhibition. HDAC6 binds both polyubiquitinated cargo and the dynein-dynactin motor complex, and it is required for the retrograde transport of ubiquitinated cargo and formation of aggresomes (18, 52). However, under conditions of proteasomal inhibition HDAC6 is also an important mediator of the autophagosomal-lysosomal pathway of protein degradation in neurons, and when overexpressed HDAC6 can rescue neurodegeneration in a fly model (16). Expression of p25α could potentially influence autophagosomal processing due to HDAC6 inhibition on several levels (see Fig. 12 for a schematic representation). First, p25α could interfere with the interactions between HDAC6 and dynactin, thereby uncoupling retrograde transport of polyubiquitinated cargo (18) and potentially autophagosomes (16). As estimated by FRAP, p25α expression severely reduced the mobility of autophagosomes, and direct inhibition of HDAC6 with trichostatin or shRNA knockdown similarly decreased mobility. We note that p62/SQSTM1-mediated retrograde transport of Htt-115Q-GFP to form conspicuous aggresomes was not disturbed by p25α expression, suggesting that hyper-acetylation of tubulin does not by itself affect retrograde transport. Second, HDAC6 has recently been pinpointed to an important role further downstream in the autophagic pathway as it deacetylates cortactin, which in turn is specifically required for fusion of QC autophagosome intermediates with lysosomes (40). This fusion event was severely affected by p25α expression, as evidenced by the following: (i) lack of co-localization between α-synuclein and LAMP1; (ii) decreased amount of α-synuclein in heavy fractions following sucrose gradient fractionation; (iii) decreased mCherry to eGFP fluorescence ratio of the LC3B fusion protein, and (iv) decreased DQ-BSA degradation, which all testify to an inhibition of autophagosomal/amphisomal fusion with lysosomes. Therefore, by several mechanisms p25α expression caused the build up of late autophagosomal elements. These likely include the multilamellar bodies observed in abundance by EM in α-synuclein$_{A30P}$/p25α-expressing cells as late endosomes and thereby amphisomes receive lysosomal hydrolases from the biosynthetic pathway to commence degradation of luminal contents.

α-Synuclein Is Secreted by Exophagy—Even though p25α imposed a partial inhibition of the degradative capacity of the cell, the turnover of α-synuclein was increased by p25α expression. We found that this phenomenon could be explained by a markedly increased secretion of α-synuclein into the external environment, and our data indicate that exocytosis of autophagosomes and amphisomes containing α-synuclein is responsible for this. In particular, amphisomes may be involved in the release of α-synuclein, as they constitute the compartment immediately preceding the p25α-mediated maturation block. Such a role also correlates well with the known physiological exocytosis of late endosomes (42), as well as the recently described unconventional secretion of the cytosolic Acb1 protein through exophagy of autophagosome intermediates in yeast (37, 53). In partial agreement with a recent report (43), we find that a small fraction (<3% of total secreted α-synuclein) of monomer α-synuclein is associated with exosomes. The significance of this is at present unclear, but secretion of exosomes represents a physiological mechanism for transferring cytosolic proteins in between cells that should be explored further in the context of disease transmission (54–56). Exosomes, however, are clearly not required to start the pathological cascade of inter-neuronal transmission of α-synuclein-derived prionoids, as α-synuclein aggregates made *in vitro* from recombinant α-synuclein is taken up by neurons in culture, and suffices to induce propagating inclusion disease in α-synuclein transgenic mice (2, 5).

Formation of autophagosomes was a prerequisite for secretion of α-synuclein. First of all, by cryo-immunogold labeling almost all vesicular α-synuclein was present in autophagosomes, amphisomes, or autolysosomes. Second, expression of

FIGURE 10. **HDAC6 inhibition mimics p25α-induced secretion of α-synuclein and reduces the mobility of autophagosomes.** *A,* representative Western blots showing cellular protein levels of acetylated tubulin (*AcTub*) and α-tubulin *(α-Tub*) obtained from PC12 cell populations as indicated. *B,* cell lysates and conditioned medium from PC12-α-synuclein$_{A30P}$ (*α-SNC$_{A30P}$*) or PC12-α-SNC$_{A30P}$/p25α cells, transduced 3 to 4 days prior to analysis with lentivectors expressing control (pLKO.1) or HDAC6-specific shRNA, were subjected to Western blotting using anti acetylated tubulin and α-tubulin antibodies (cell lysates) or anti-α-SNC antibodies (TCA-precipitated medium; BD Transduction Laboratories). Integrated optical density (*IOD*) of western bands for acetylated tubulin in cell lysates (*C*) and secreted α-SNC (BD Transduction Laboratories) in the TCA samples (*D*) is presented as fold increase relative to untreated control cells. Mean ± S.E. of three independent experiments are shown. * denotes a statistically significant increase in IOD within the cell line when co-expressing shRNA, and # denotes a statistic significant increase in IOD between the control cell lines not expressing shRNA. *E,* cell lysates of PC12 cell populations as indicated, expressing mCherry-eGFP-LC3B were Western blotted with anti-GFP antibodies to demonstrate an equal expression of the LC3B fusion protein. The 72-kDa protein bands correspond to the size of the mCherry-eGFP-LC3B tandem construct. *F,* flow cytometric analysis of untreated or trichostatin A-treated (10 μM) PC12 cell populations expressing mCherry-eGFP-LC3B. The *bar graph* shows mean ± S.E. of eGFP relative light fluorescent units normalized to control cells expressing β-SNC and represents data from three independent experiments. * denotes a statistic significant increase in mean eGFP fluorescence intensity between the cell lines when compared with β-SNC-expressing PC12 cells, and # denotes a statistic significant increase after trichostatin treatment. *A.U.*, arbitrary units. *G* and *H,* live cell confocal microscopy images of PC12 cells expressing β-SNC or α-SNC$_{A30P}$/p25α showing FRAP time series before and after photobleaching ($t = 0$ s and $t = 50$ s), and after a defined recovery period ($t = 260$ s). The cells were bleached in the encircled ROI shown in close-ups just before the $t = 50$-s time point. *Bars,* 10 μm. *I, bar graph* shows percentage of FRAP in PC12 cells as indicated, including PC12-α-SNC$_{A30P}$ cells treated with 20 μM trichostatin A or transduced with HDAC6 shRNA. Mean ± S.E. were obtained from three to five independent experiments. * denotes a statistically significant decrease in FRAP between the cell lines when compared with β-SNC-expressing PC12 cells, and # denotes a statistically significant decrease after trichostatin treatment or HDAC6 shRNA co-expression when compared with PC12 cells expressing α-SNC$_{A30P}$.

p25α correlated with increased levels of phosphatidylserine on the plasma membrane in the absence of apoptosis, indicative of exocytosis of late endosome/amphisome elements. Finally, secretion of α-synuclein could be controlled by chemical or genetic modulation of autophagy initiation (trehalose, 3-MA, and Rab1), elongation (ATG5 shRNA), or autophagosome maturation (bafilomycin). Knockdown or introduction of mutants of Rab27A, which regulates fusion of late endosomes with the

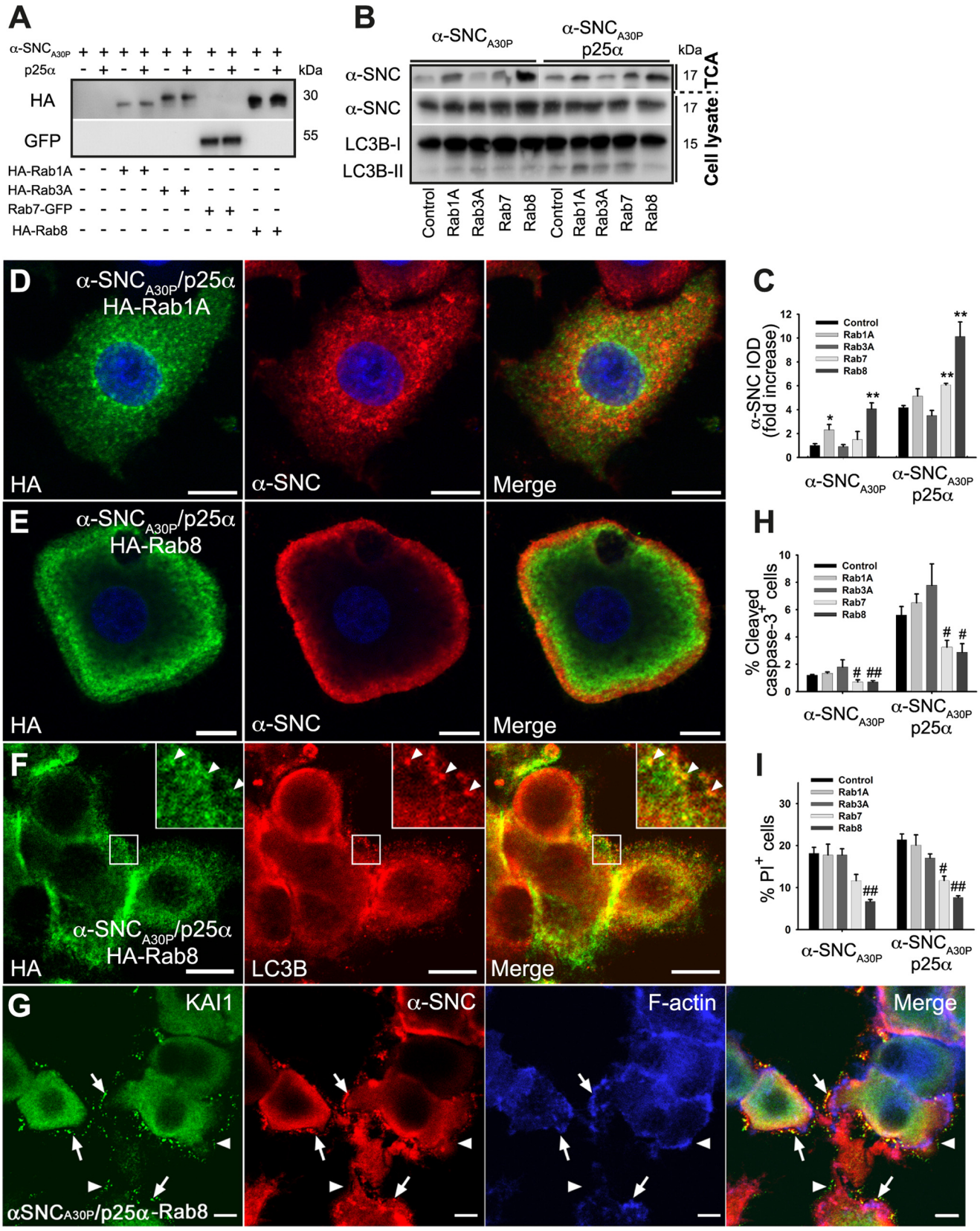

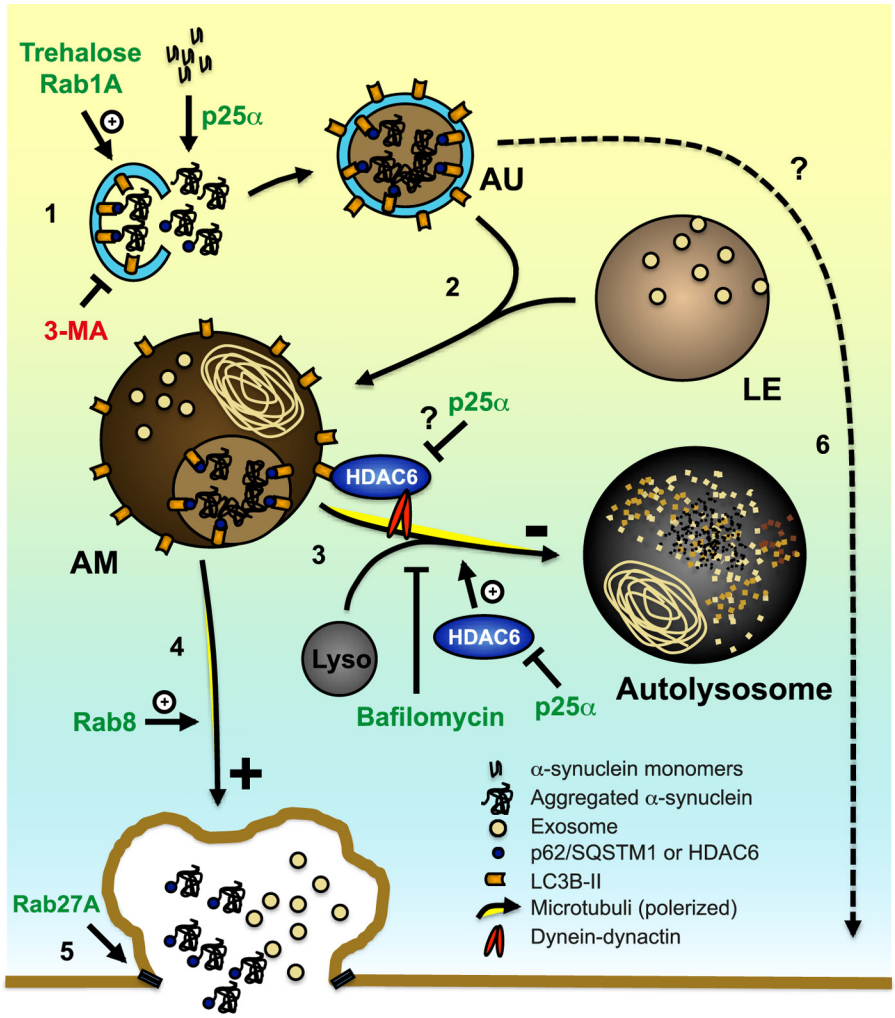

FIGURE 12. **Proposed mechanism for p25α effects and exophagy of α-synuclein.** The diagram illustrates how p25α may alter trafficking pathways (marked by *numbers*) and autophagosome dynamics. Expression of p25α causes aggregation and autophagosomal uptake of α-synuclein (*α-SNC*), involving QC autophagosome adaptors p62/SQSTM1 and possibly HDAC6 (*1*). The autophagosome (*AU*) then fuses (*2*) with a late endosome (*LE*) to generate an amphisome (*AM*), which can travel retrogradely (*3*) to fuse with a lysosome (*Lyso*) thereby forming an autolysosome, which degrades α-SNC. Retrograde transport involves HDAC6-mediated interactions between LC3B and the minus-end-directed dynein-dynactin motor complex, which may be inhibited by p25α. Fusion of amphisomes with lysosomes is promoted by HDAC6 deacetylase activity, which is inhibited by p25α. Under conditions where pathway *3* is blocked (compromised HDAC6 activity, lysosomal dysfunction, and/or altered ratio of minus- to plus-end-directed trafficking of amphisomes), anterograde transport of amphisomes toward the cell surface takes place (*4*), where a fraction of competent amphisomes can undergo exocytosis regulated by Rab27A (*5*), to release α-SNC in monomer and aggregated/modified forms to the extracellular environment. The extent to which autophagosomes may directly contribute to exocytosis is unclear (*6*).

plasma membrane (44), in PC12 α-synuclein$_{A30P}$/p25α cells was problematic in terms of cell death, but expression of Rab27A dominant positive and negative mutants in PC12-α-synuclein$_{A30P}$ cells modulated the release of α-synuclein. In addition, the fact that α-synuclein$_{A30P}$ was also present in autophagosomes in the absence of p25α expression and that the basal release of α-synuclein in PC12-α-synuclein$_{A30P}$ cells was up-regulated by trehalose (and Rab1A, Rab8, or HDAC6

FIGURE 11. **Expression of Rab8 enhances α-synuclein secretion while lowering cell death.** *A,* representative Western blots showing expression levels of HA-tagged Rab1A, Rab3A, or Rab8 and GFP-tagged Rab7 in PC12 cell lines expressing α-synuclein$_{A30P}$ (*α-SNC$_{A30P}$*) or α-SNC$_{A30P}$ and p25α using anti-HA or -GFP antibodies. *B,* representative Western blots of TCA-precipitated media and cell lysates obtained from PC12 cells expressing α-SNC$_{A30P}$ or α-SNC$_{A30P}$/p25α with or without co-expression of Rab proteins as indicated using antibodies against α-SNC (BD Transduction Laboratories) and LC3B. *C,* quantified integrated optical density (*IOD*) of α-SNC Western blot bands obtained in *B* are presented as fold increase relative to α-SNC$_{A30P}$-expressing PC12 cells. Mean ± S.E. of five independent experiments are shown. * denotes a statistic significant increase in IOD when compared with control cells within the respective cell line. *D–F,* indirect immunofluorescence of PC12-α-SNC$_{A30P}$/p25α cells co-expressing either HA-Rab1A (*D*) or HA-Rab8 (*E* and *F*). Rab8 was predominantly distributed toward the cell surface and caused a more peripheral distribution of α-SNC$_{A30P}$ (BD Transduction Laboratories) (*E*) and was co-localized partly with LC3B-positive autophagosomes/amphisomes (*F*). *Bars,* 10 μm. *G,* PC12-α-SNC$_{A30P}$/p25α cells co-expressing HA-tagged Rab8 were fixed after 2 days of transgene induction and then processed for immunofluorescence to visualize KAI1 (*green*), α-SNC (*red*), or F-actin detected with Alexa 633-conjugated phalloidin (*blue*). Note that Rab8 expression results in accumulation of material on the cell surface, which is immunoreactive with anti-α-SNC and KAI1 antibodies (*arrows*). The figure is representative of three independent experiments. *Bars,* 10 μm. *H, bar graph* shows the percentage of caspase-3-positive PC12 cells of the whole population in indicated cell populations as determined by indirect immunofluorescence and counting. Data represent mean ± S.E. of four independent experiments. *I,* flow cytometric analysis of PC12 cell populations as indicated stained with PI to measure cell death. The *bar graph* shows the percentage of PI-positive cells of the total population and represents mean ± S.E. of four independent experiments. *H* and *I,* # denotes a statistically significant decrease when compared with control cells within the same cell line.

shRNA), indicates that exophagy of α-synuclein is a mechanism that is likely operational also in the absence of p25α expression. Exophagy was specific for α-synuclein inasmuch as co-expressed Htt-115Q-GFP was not taken up into autophagosomes and was only to a minor degree secreted into the medium. Both early and late endosomes can fuse with newly formed autophagosomes to form amphisomes (57). Recently, it was reported that interference with VPS4 function, required for formation of late endosomes, caused secretion of α-synuclein potentially through elements of the early endosomal pathway (58), but whether this involved exocytosis of early amphisomal elements is unknown.

The Rab family of small GTPases constitutes important regulators of biosynthetic and endosomal vesicular trafficking. Rab1A or Rab8 have been shown to rescue α-synuclein-induced cytotoxicity in small organism models, possibly by alleviating endoplasmic reticulum-to-Golgi transport deficits induced by α-synuclein expression (45, 46). However, Rab8 also facilitates polarized vesicular transport toward the plasma membrane (59–61). When overexpressed in PC12 cells, Rab8 caused a pronounced redistribution of $\alpha\text{-synuclein}_{A30P}$ elements to the plasma membrane, which was accompanied by a significantly increased secretion of α-synuclein with or without p25α expression. Rab1A also increased α-synuclein secretion in PC12 cells expressing only $\alpha\text{-synuclein}_{A30P}$ likely reflecting the reported role of Rab1A in autophagy initiation (36). Rab7 regulates dynamics and fusion events of late endosomal and autophagosomal elements (48, 49, 62). However, Rab7 overexpression did not circumvent the p25α-imposed fusion block and instead increased the secretion of α-synuclein, potentially as a consequence of Rab7-promoted plus-end-directed microtubular transport of amphisomes through interactions with the LC3B-binding protein FYCO (63). Secretion of cytotoxic α-synuclein might be beneficial for the individual neuron as both Rab7 and Rab8, which promoted secretion, also reduced mortality significantly. However, secretion of α-synuclein may be a pathological mechanism of PD pathology transmission to nearby neurons (2, 3, 7), and in addition it can activate resident microglia, which mediate neuroinflammation and thereby exacerbate disease progression (64–66).

In conclusion, we propose that exophagy, with or without ectopic expression of p25α, may be an important physiological mechanism for unconventional secretion of α-synuclein from dopaminergic neurons, and we predict that lysosomal dysfunction observed in neurodegenerative diseases including PD (50) will aggravate such a release.

Acknowledgments—We are greatly indebted to Mette Ohlsen for expert help with EM and to colleagues for their generous help as mentioned.

REFERENCES

1. Braak, H., Del Tredici, K., Rüb, U., de Vos, R. A., Jansen Steur, E. N., and Braak, E. (2003) Staging of brain pathology related to sporadic Parkinson disease. *Neurobiol. Aging* **24,** 197–211
2. Luk, K. C., Kehm, V. M., Zhang, B., O'Brien, P., Trojanowski, J. Q., and Lee, V. M. (2012) Intracerebral inoculation of pathological α-synuclein initiates a rapidly progressive neurodegenerative α-synucleinopathy in mice. *J. Exp. Med.* **209,** 975–986
3. Desplats, P., Lee, H. J., Bae, E. J., Patrick, C., Rockenstein, E., Crews, L., Spencer, B., Masliah, E., and Lee, S. J. (2009) Inclusion formation and neuronal cell death through neuron-to-neuron transmission of α-synuclein. *Proc. Natl. Acad. Sci. U.S.A.* **31,** 13010–13015
4. Lee, H. J., Patel, S., and Lee, S. J. (2005) Intravesicular localization and exocytosis of α-synuclein and its aggregates. *J. Neurosci.* **25,** 6016–6024
5. Volpicelli-Daley, L. A., Luk, K. C., Patel, T. P., Tanik, S. A., Riddle, D. M., Stieber, A., Meaney, D. F., Trojanowski, J. Q., and Lee, V. M. (2011) Exogenous α-synuclein fibrils induce Lewy body pathology leading to synaptic dysfunction and neuron death. *Neuron* **72,** 57–71
6. Kordower, J. H., Chu, Y., Hauser, R. A., Freeman, T. B., and Olanow, C. W. (2008) Lewy body-like pathology in long-term embryonic nigral transplants in Parkinson disease. *Nat. Med.* **14,** 504–506
7. Hansen, C., Angot, E., Bergström, A. L., Steiner, J. A., Pieri, L., Paul, G., Outeiro, T. F., Melki, R., Kallunki, P., Fog, K., Li, J. Y., and Brundin, P. (2011) α-Synuclein propagates from mouse brain to grafted dopaminergic neurons and seeds aggregation in cultured human cells. *J. Clin. Invest.* **121,** 715–725
8. Vogiatzi, T., Xilouri, M., Vekrellis, K., and Stefanis, L. (2008) Wild type α-synuclein is degraded by chaperone-mediated autophagy and macroautophagy in neuronal cells. *J. Biol. Chem.* **283,** 23542–23556
9. Webb, J. L., Ravikumar, B., Atkins, J., Skepper, J. N., and Rubinsztein, D. C. (2003) α-Synuclein is degraded by both autophagy and the proteasome. *J. Biol. Chem.* **278,** 25009–25013
10. Kraft, C., Peter, M., and Hofmann, K. (2010) Selective autophagy: ubiquitin-mediated recognition and beyond. *Nat. Cell Biol.* **12,** 836–841
11. Tooze, S. A., and Yoshimori, T. (2010) The origin of the autophagosomal membrane. *Nat. Cell Biol.* **12,** 831–835
12. Xie, Z., and Klionsky, D. J. (2007) Autophagosome formation: core machinery and adaptations. *Nat. Cell Biol.* **9,** 1102–1109
13. Mehrpour, M., Esclatine, A., Beau, I., and Codogno, P. (2010) Overview of macroautophagy regulation in mammalian cells. *Cell* **20,** 748–762
14. Fader, C. M., and Colombo, M. I. (2009) Autophagy and multivesicular bodies: two closely related partners. *Cell Death Differ.* **16,** 70–78
15. Komatsu, M., Waguri, S., Koike, M., Sou, Y. S., Ueno, T., Hara, T., Mizushima, N., Iwata, J., Ezaki, J., Murata, S., Hamazaki, J., Nishito, Y., Iemura, S., Natsume, T., Yanagawa, T., Uwayama, J., Warabi, E., Yoshida, H., Ishii, T., Kobayashi, A., Yamamoto, M., Yue, Z., Uchiyama, Y., Kominami, E., and Tanaka, K. (2007) Homeostatic levels of p62 control cytoplasmic inclusion body formation in autophagy-deficient mice. *Cell* **131,** 1149–1163
16. Pandey, U. B., Nie, Z., Batlevi, Y., McCray, B. A., Ritson, G. P., Nedelsky, N. B., Schwartz, S. L., DiProspero, N. A., Knight, M. A., Schuldiner, O., Padmanabhan, R., Hild, M., Berry, D. L., Garza, D., Hubbert, C. C., Yao, T. P., Baehrecke, E. H., and Taylor, J. P. (2007) HDAC6 rescues neurodegeneration and provides an essential link between autophagy and the UPS. *Nature* **447,** 859–863
17. Gamerdinger, M., Hajieva, P., Kaya, A. M., Wolfrum, U., Hartl, F. U., and Behl, C. (2009) Protein quality control during aging involves recruitment of the macroautophagy pathway by BAG3. *EMBO J.* **28,** 889–901
18. Kawaguchi, Y., Kovacs, J. J., McLaurin, A., Vance, J. M., Ito, A., and Yao, T. P. (2003) The deacetylase HDAC6 regulates aggresome formation and cell viability in response to misfolded protein stress. *Cell* **115,** 727–738
19. Komatsu, M., Kurokawa, H., Waguri, S., Taguchi, K., Kobayashi, A., Ichimura, Y., Sou, Y. S., Ueno, I., Sakamoto, A., Tong, K. I., Kim, M., Nishito, Y., Iemura, S., Natsume, T., Ueno, T., Kominami, E., Motohashi, H., Tanaka, K., and Yamamoto, M. (2010) The selective autophagy substrate p62 activates the stress responsive transcription factor Nrf2 through inactivation of Keap1. *Nat. Cell Biol.* **12,** 213–223
20. Pankiv, S., Clausen, T. H., Lamark, T., Brech, A., Bruun, J. A., Outzen, H., Øvervatn, A., Bjørkøy, G., and Johansen, T. (2007) p62/SQSTM1 binds directly to Atg8/LC3 to facilitate degradation of ubiquitinated protein aggregates by autophagy. *J. Biol. Chem.* **282,** 24131–24145
21. Komatsu, M., Waguri, S., Chiba, T., Murata, S., Iwata, J., Tanida, I., Ueno, T., Koike, M., Uchiyama, Y., Kominami, E., and Tanaka, K. (2006) Loss of autophagy in the central nervous system causes neurodegeneration in mice. *Nature* **441,** 880–884
22. Xie, Y. Y., Zhou, C. J., Zhou, Z. R., Hong, J., Che, M. X., Fu, Q. S., Song,

A. X., Lin, D. H., and Hu, H. Y. (2010) Interaction with synphilin-1 promotes inclusion formation of α-synuclein: mechanistic insights and pathological implication. *FASEB J.* **24,** 196–205
23. Ryo, A., Togo, T., Nakai, T., Hirai, A., Nishi, M., Yamaguchi, A., Suzuki, K., Hirayasu, Y., Kobayashi, H., Perrem, K., Liou, Y. C., and Aoki, I. (2006) Prolyl-isomerase Pin1 accumulates in Lewy bodies of Parkinson disease and facilitates formation of α-synuclein inclusions. *J. Biol. Chem.* **281,** 4117–4125
24. Lindersson, E., Lundvig, D., Petersen, C., Madsen, P., Nyengaard, J. R., Højrup, P., Moos, T., Otzen, D., Gai, W. P., Blumbergs, P. C., and Jensen, P. H. (2005) p25α stimulates α-synuclein aggregation and is co-localized with aggregated α-synuclein in α-synucleinopathies. *J. Biol. Chem.* **280,** 5703–5715
25. Acevedo, K., Li, R., Soo, P., Suryadinata, R., Sarcevic, B., Valova, V. A., Graham, M. E., Robinson, P. J., and Bernard, O. (2007) The phosphorylation of p25/TPPP by LIM kinase 1 inhibits its ability to assemble microtubules. *Exp. Cell Res.* **313,** 4091–4106
26. Tirián, L., Hlavanda, E., Oláh, J., Horváth, I., Orosz, F., Szabó, B., Kovács, J., Szabad, J., and Ovádi, J. (2003) TPPP/p25 promotes tubulin assemblies and blocks mitotic spindle formation. *Proc. Natl. Acad. Sci. U.S.A.* **100,** 13976–13981
27. Tokési, N., Lehotzky, A., Horváth, I., Szabó, B., Oláh, J., Lau, P., and Ovádi, J. (2010) TPPP/p25 promotes tubulin acetylation by inhibiting histone deacetylase 6. *J. Biol. Chem.* **285,** 17896–17906
28. Kragh, C. L., Lund, L. B., Febbraro, F., Hansen, H. D., Gai, W. P., El-Agnaf, O., Richter-Landsberg, C., and Jensen, P. H. (2009) α-Synuclein aggregation and Ser-129 phosphorylation-dependent cell death in oligodendroglial cells. *J. Biol. Chem.* **284,** 10211–10222
29. Goldbaum, O., Jensen, P. H., and Richter-Landsberg, C. (2008) The expression of tubulin polymerization promoting protein TPPP/p25α is developmentally regulated in cultured rat brain oligodendrocytes and affected by proteolytic stress. *Glia* **56,** 1736–1746
30. Yokoyama, K., Kaji, H., He, J., Tanaka, C., Hazama, R., Kamigaki, T., Ku, Y., Tohyama, K., and Tohyama, Y. (2011) Rab27a negatively regulates phagocytosis by prolongation of the actin-coating stage around phagosomes. *J. Biol. Chem.* **286,** 5375–5382
31. Hasholt, L., Abell, K., Nørremølle, A., Nellemann, C., Fenger, K., and Sørensen, S. A. (2003) Antisense down-regulation of mutant huntingtin in a cell model. *J. Gene Med.* **5,** 528–538
32. Vilhardt, F., Plastre, O., Sawada, M., Suzuki, K., Wiznerowicz, M., Kiyokawa, E., Trono, D., and Krause, K.-H. (2002) The HIV-1 Nef protein and phagocyte NADPH oxidase activation. *J. Biol. Chem.* **277,** 42136–42143
33. Vilhardt, F., Nielsen, M., Sandvig, K., and van Deurs, B. (1999) Urokinase-type plasminogen activator receptor is internalized by different mechanisms in polarized and nonpolarized Madin-Darby canine kidney epithelial cells. *Mol. Biol. Cell* **10,** 179–195
34. Cuervo, A. M., Stefanis, L., Fredenburg, R., Lansbury, P. T., and Sulzer, D. (2004) Impaired degradation of mutant α-synuclein by chaperone-mediated autophagy. *Science* **305,** 1292–1295
35. Martinez-Vicente, M., Talloczy, Z., Kaushik, S., Massey, A. C., Mazzulli, J., Mosharov, E. V., Hodara, R., Fredenburg, R., Wu, D. C., Follenzi, A., Dauer, W., Przedborski, S., Ischiropoulos, H., Lansbury, P. T., Sulzer, D., and Cuervo, A. M. (2008) Dopamine-modified α-synuclein blocks chaperone-mediated autophagy. *J. Clin. Invest.* **118,** 777–788
36. Winslow, A. R., Chen, C. W., Corrochano, S., Acevedo-Arozena, A., Gordon, D. E., Peden, A. A., Lichtenberg, M., Menzies, F. M., Ravikumar, B., Imarisio, S., Brown, S., O'Kane, C. J., and Rubinsztein, D. C. (2010) α-Synuclein impairs macroautophagy: implications for Parkinson disease. *J. Cell Biol.* **190,** 1023–1037
37. Manjithaya, R., and Subramani, S. (2011) Autophagy: a broad role in unconventional protein secretion? *Trends Cell Biol.* **21,** 67–73
38. Wu, Y. T., Tan, H. L., Shui, G., Bauvy, C., Huang, Q., Wenk, M. R., Ong, C. N., Codogno, P., and Shen, H. M. (2010) Dual role of 3-methyladenine in modulation of autophagy via different temporal patterns of inhibition on class I and III phosphoinositide 3-kinase. *J. Biol. Chem.* **285,** 10850–10861
39. Sarkar, S., Davies, J. E., Huang, Z., Tunnacliffe, A., and Rubinsztein, D. C. (2007) Trehalose, a novel mTOR-independent autophagy enhancer, accelerates the clearance of mutant huntingtin and α-synuclein. *J. Biol. Chem.* **282,** 5641–5652
40. Lee, J. Y., Koga, H., Kawaguchi, Y., Tang, W., Wong, E., Gao, Y. S., Pandey, U. B., Kaushik, S., Tresse, E., Lu, J., Taylor, J. P., Cuervo, A. M., and Yao, T. P. (2010) HDAC6 controls autophagosome maturation essential for ubiquitin-selective quality-control autophagy. *EMBO J.* **29,** 969–980
41. Demo, S. D., Masuda, E., Rossi, A. B., Throndset, B. T., Gerard, A. L., Chan, E. H., Armstrong, R. J., Fox, B. P., Lorens, J. B., Payan, D. G., Scheller, R. H., and Fisher, J. M. (1999) Quantitative measurement of mast cell degranulation using a novel flow cytometric annexin-V binding assay. *Cytometry* **36,** 340–348
42. Denzer, K., Kleijmeer, M. J., Heijnen, H. F., Stoorvogel, W., and Geuze, H. J. (2000) Exosome: from internal vesicle of the multivesicular body to intercellular signaling device. *J. Cell Sci.* **113,** 3365–3374
43. Emmanouilidou, E., Melachroinou, K., Roumeliotis, T., Garbis, S. D., Ntzouni, M., Margaritis, L. H., Stefanis, L., and Vekrellis, K. (2010) Cell-produced α-synuclein is secreted in a calcium-dependent manner by exosomes and impacts neuronal survival. *J. Neurosci.* **30,** 6838–6851
44. Ostrowski, M., Carmo, N. B., Krumeich, S., Fanget, I., Raposo, G., Savina, A., Moita, C. F., Schauer, K., Hume, A. N., Freitas, R. P., Goud, B., Benaroch, P., Hacohen, N., Fukuda, M., Desnos, C., Seabra, M. C., Darchen, F., Amigorena, S., Moita, L. F., and Thery, C. (2010) Rab27a and Rab27b control different steps of the exosome secretion pathway. *Nat. Cell Biol.* **12,** 19–30
45. Cooper, A. A., Gitler, A. D., Cashikar, A., Haynes, C. M., Hill, K. J., Bhullar, B., Liu, K., Xu, K., Strathearn, K. E., Liu, F., Cao, S., Caldwell, K. A., Caldwell, G. A., Marsischky, G., Kolodner, R. D., Labaer, J., Rochet, J. C., Bonini, N. M., and Lindquist, S. (2006) α-Synuclein blocks ER-Golgi traffic and Rab1 rescues neuron loss in Parkinson models. *Science* **313,** 324–328
46. Gitler, A. D., Bevis, B. J., Shorter, J., Strathearn, K. E., Hamamichi, S., Su, L. J., Caldwell, K. A., Caldwell, G. A., Rochet, J. C., McCaffery, J. M., Barlowe, C., and Lindquist, S. (2008) The Parkinson disease protein α-synuclein disrupts cellular Rab homeostasis. *Proc. Natl. Acad. Sci. U.S.A.* **105,** 145–150
47. Yeger-Lotem, E., Riva, L., Su, L. J., Gitler, A. D., Cashikar, A. G., King, O. D., Auluck, P. K., Geddie, M. L., Valastyan, J. S., Karger, D. R., Lindquist, S., and Fraenkel, E. (2009) Bridging high-throughput genetic and transcriptional data reveals cellular responses to α-synuclein toxicity. *Nat. Genet.* **41,** 316–323
48. Bucci, C., Thomsen, P., Nicoziani, P., McCarthy, J., and van Deurs, B. (2000) Rab7: a key to lysosome biogenesis. *Mol. Biol. Cell* **11,** 467–480
49. Jäger, S., Bucci, C., Tanida, I., Ueno, T., Kominami, E., Saftig, P., and Eskelinen, E. L. (2004) Role for Rab7 in maturation of late autophagic vacuoles. *J. Cell Sci.* **117,** 4837–4848
50. Dehay, B., Bové, J., Rodríguez-Muela, N., Perier, C., Recasens, A., Boya, P., and Vila, M. (2010) Pathogenic lysosomal depletion in Parkinson disease. *J. Neurosci.* **30,** 12535–12544
51. Mak, S. K., McCormack, A. L., Manning-Bog, A. B., Cuervo, A. M., and Di Monte, D. A. (2010) Lysosomal degradation of α-synuclein *in vivo*. *J. Biol. Chem.* **285,** 13621–13629
52. Olzmann, J. A., Li, L., Chudaev, M. V., Chen, J., Perez, F. A., Palmiter, R. D., and Chin, L. S. (2007) Parkin-mediated K63-linked polyubiquitination targets misfolded DJ-1 to aggresomes via binding to HDAC6. *J. Cell Biol.* **178,** 1025–1038
53. Duran, J. M., Anjard, C., Stefan, C., Loomis, W. F., and Malhotra, V. (2010) Unconventional secretion of Acb1 is mediated by autophagosomes. *J. Cell Biol.* **188,** 527–536
54. Schneider, A., and Simons, M. (2013) Exosomes: vesicular carriers for intercellular communication in neurodegenerative disorders. *Cell Tissue Res.* **352,** 33–47
55. Koles, K., Nunnari, J., Korkut, C., Barria, R., Brewer, C., Li, Y., Leszyk, J., Zhang, B., and Budnik, V. (2012) Mechanism of evenness interrupted (Evi)-exosome release at synaptic boutons. *J. Biol. Chem.* **287,** 16820–16834
56. Korkut, C., Ataman, B., Ramachandran, P., Ashley, J., Barria, R., Gherbesi, N., and Budnik, V. (2009) Trans-synaptic transmission of vesicular Wnt signals through Evi/Wntless. *Cell* **139,** 393–404

57. Liou, W., Geuze, H. J., Geelen, M. J., and Slot, J. W. (1997) The autophagic and endocytic pathways converge at the nascent autophagic vacuoles. *J. Cell Biol.* **136,** 61–70
58. Hasegawa, T., Konno, M., Baba, T., Sugeno, N., Kikuchi, A., Kobayashi, M., Miura, E., Tanaka, N., Tamai, K., Furukawa, K., Arai, H., Mori, F., Wakabayashi, K., Aoki, M., Itoyama, Y., and Takeda, A. (2011) The AAA-ATPase VPS4 regulates extracellular secretion and lysosomal targeting of α-synuclein. *PLoS One* **6,** e29460
59. Bravo-Cordero, J. J., Marrero-Diaz, R., Megías, D., Genís, L., García-Grande, A., García, M. A., Arroyo, A. G., and Montoya, M. C. (2007) MT1-MMP proinvasive activity is regulated by a novel Rab8-dependent exocytic pathway. *EMBO J.* **26,** 1499–1510
60. Hattula, K., Furuhjelm, J., Tikkanen, J., Tanhuanpää, K., Laakkonen, P., and Peränen, J. (2006) Characterization of the Rab8-specific membrane traffic route linked to protrusion formation. *J. Cell Sci.* **119,** 4866–4877
61. Sato, T., Mushiake, S., Kato, Y., Sato, K., Sato, M., Takeda, N., Ozono, K., Miki, K., Kubo, Y., Tsuji, A., Harada, R., and Harada, A. (2007) The Rab8 GTPase regulates apical protein localization in intestinal cells. *Nature* **448,** 366–369
62. Lebrand, C., Corti, M., Goodson, H., Cosson, P., Cavalli, V., Mayran, N., Fauré, J., and Gruenberg, J. (2002) Late endosome motility depends on lipids via the small GTPase Rab7. *EMBO J.* **21,** 1289–1300
63. Pankiv, S., Alemu, E. A., Brech, A., Bruun, J. A., Lamark, T., Overvatn, A., Bjørkøy, G., and Johansen, T. (2010) FYCO1 is a Rab7 effector that binds to LC3 and PI3P to mediate microtubule plus end-directed vesicle transport. *J. Cell Biol.* **188,** 253–269
64. Block, M. L., Zecca, L., and Hong, J. S. (2007) Microglia-mediated neurotoxicity: uncovering the molecular mechanisms. *Nat. Rev. Neurosci.* **8,** 57–69
65. Zhang, W., Dallas, S., Zhang, D., Guo, J. P., Pang, H., Wilson, B., Miller, D. S., Chen, B., Zhang, W., McGeer, P. L., Hong, J. S., and Zhang, J. (2007) Microglial PHOX and Mac-1 are essential to the enhanced dopaminergic neurodegeneration elicited by A30P and A53T mutant α-synuclein. *Glia* **55,** 1178–1188
66. Zhang, W., Wang, T., Pei, Z., Miller, D. S., Wu, X., Block, M. L., Wilson, B., Zhang, W., Zhou, Y., Hong, J. S., and Zhang, J. (2005) Aggregated α-synuclein activates microglia: a process leading to disease progression in Parkinson disease. *FASEB J.* **19,** 533–542